國立台灣大學生命科學院生命科學系

碩士論文

Department of Life Science

College of Life Science

National Taiwan University

Master Thesis

基質金屬蛋白酶在瓢體蟲 *Aeolosoma viride* 前端再生扮演的角色

The roles of matrix metalloproteinases in anterior regeneration in *Aeolosoma viride*

曾子倫

Tzu-Lun Tseng

指導教授：陳俊宏 博士

Advisor: Jiun-Hong Chen, Ph. D.

中華民國 105 年 7 月

July, 2016

國立臺灣大學碩士學位論文
口試委員會審定書

基質金屬蛋白酶在瓢體蟲 Aeolosoma viride 前端再生扮演的角色

The roles of matrix metalloproteinases in anterior regeneration in *Aeolosoma viride*

本論文係曾子倫君（R03B21001）在國立臺灣大學生命科學學系、所完成之碩士學位論文，於民國 105 年 7 月 4 日承下列考試委員審查通過及口試及格，特此證明

口試委員：

陳俊彥 　　（簽名）
（指導教授）

牛家蕓 　　郭典翰

生命科學系 系主任 　閱台三峰　（簽名）

i

致謝

在寫這篇碩士論文的時候我有了非常多的感觸,受到了很多人的幫助,像是陳俊宏老師花很多心力幫助我修改我的文筆,以及實驗邏輯,而郭典翰老師會跟我討論我的實驗,並告訴了我很多他的經驗談,讓我學到了很多東西,朱家瑩老師也會指出我論文中不足的地方,並提供我可能的解決方法。在實驗室中同學們和助理也會督促我去寫我的論文。而由於我在撰寫論文的同時也參加了很多研討會、比賽及演講,很感謝實驗室的同學際帆和其嶸以及學妹紘瑜幫我聽我的預講,在幾次的演練中,他們應該已經聽到爛了,但還是會很認真地聽完並給予我建議。

而在整個碩士班的期間,我也受到很多人幫助,尤其在生科館大停電的期間,很多同學在我詢問借用冰箱的時候,都二話不說的就挪出空間讓我們轉移我們冰箱裡的東西,讓我非常的感動。而生科館的同學們也常協助我的實驗、助教課及研究,嬿涵、思卉和偉民提供的幫忙尤其多,因此在此特別提出感謝。也感謝郭典翰老師借我顯微鏡照相、李士傑老師借我顯微注射儀及李心予老師借我藥品及細胞進行實驗。Techcomm 中心內的技術員的幫助、儀器的借用及教學。

最後,雖然這篇論文並未達到我本來的預期,但在這期間我學到很多,也藉由很多機會鍛鍊自己,所以我要感謝我的家人,他們提供了我許多支持,讓我得以無後顧之憂得向前邁進。
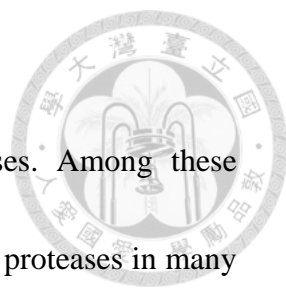
中文摘要

蛋白酶參與在生物體內許多重要的生理機制，像是消化、凝血及組織重組等。而在眾多蛋白酶中，金屬蛋白酶是一群具有最多元酵素功能的蛋白酶，其中基質金屬蛋白酶(Matrix metalloproteinase, MMP)、ADAM 及 ADAMST 為金屬蛋白酶中主要的三個類群，他們都需要金屬離子的協助才能具有正常的酵素活性。而MMP 是目前具有最多研究的金屬蛋白酶，他們是主要調控細胞外間質(Extracellular matrix)的分解及構成，已被發現參與在發育及再生過程中的細胞增生及移動。雖然在斑馬魚及渦蟲中 MMP 已被發現參與再生的過程，但 MMP 在再生中的機制仍不甚清楚。由於淡水生的環節動物瓢體蟲 (*Aeolosoma viride*) 具有很強的再生能力，並且使用和脊椎動物類似的機制來進行再生，因此在此篇研究中被用來進行 MMP 與再生的研究。在此論文的研究結果中，選殖出瓢體蟲中三種基質金屬蛋白酶，其中兩種是鑲嵌在膜上的 MMP (MT-MMP)而另外一種是分泌型的 MMP。其中兩種 MMP 在再生早期會高量表現於新生成的組織中，顯示該兩種 MMP 可能參與在再生的早期過程。進一步去檢測在再生過程中 MMP的活性變化，發現到 MMP 在再生 24 小時的時候會在新再生組織中具有很高的酵素活性。再以 MMP 活性的抑制劑 GM6001 去抑制在再生中 MMP 的活性，來了解 MMP 在再生過程中的功能，發現到只有在再生 0-12 小時內抑制酵素活性會顯著地降低再生的成功率。依據這些結果都確實 MMP 參與了瓢體蟲的早期頭部再生。
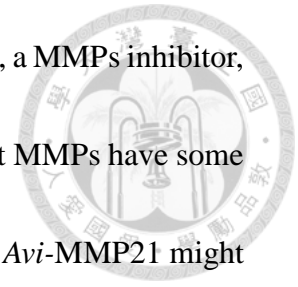
關鍵詞：瓢體蟲、再生、基質金屬蛋白酶、GM6001

Abstract

Proteases play important roles in many biological processes. Among these proteases, metalloproteases represent the largest catalytic classes of proteases in many organisms. The three major classes of metalloproteinases are ADAMs (a disintegrin and metalloproteinase domain), ADAMTS (ADAMs with thrombospondin domain), and MMP (matrix metalloproteinase). MMPs play key roles in turnover of extracellular matrix (ECM) and serve as important regulators of cell-ECM interaction during development and regeneration. Although MMPs were found involved in the regeneration in planarian and zebrafish, there is a knowledge gap between planarian and vertebrates. Therefore, the annelid was chosen to fill the gap due to the similarity of regenerative mechanism to vertebrate. In this study, a fresh water annelid with high regenerative ability, *Aeolosoma viride*, was used to solve this question. In the NGS transcriptome data of *A. viride*, three MMPs, named as *Avi*-MMP14, *Avi*-MMP21 and *Avi*-MMP17, and one MMP-like gene, *Avi*-MMP-like gene, were found. Gene expression of *Avi-mmp21* and *Avi-mmp17* significantly increased at the early stage of anterior regeneration. And, gene expression of *Avi-mmp-like gene* significantly increased at the late stage of anterior regeneration. However, *Avi-mmp14* showed no differences in expression during anterior regeneration. On the other hand, SDS-PAGE gelatin zymography showed the highest protease activity was detected at 24 hours post

amputation (hpa) blastema. Furthermore, after treated with GM6001, a MMPs inhibitor,

at 0-12 hpa, regeneration was inhibited. These results suggested that MMPs have some

effects on early stage of anterior regeneration, and *Avi*-MMP17 and *Avi*-MMP21 might

be the key factors in this processes. The relationship between MMPs and the regulation

of MMPs needs further research to be resolved.

Keywords: *Aeolosoma viride*, regeneration, matrix metalloproteinases, GM6001

Context

Introduction

Protease

Proteases are a group of enzymes that can break long peptide chains into small peptide fragments and even into single amino acid (Neitzel, 2010). They are involved in many biological processes. For example, enzymes in the intestine can digest various kinds of food. In the coagulation, the proteolytic cascade is mediated by a series of proteases. Proteases are also involved in many cellular signaling processes, such as those in apoptosis,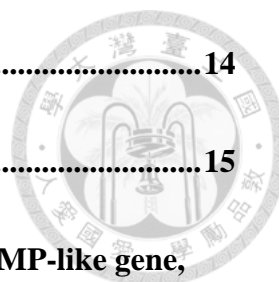 DNA replication and cell differentiation (Clark, 2001). In metazoans, proteolytic systems play important roles in tissue homeostasis, embryonic development, wound healing, and also regeneration (Clark, 2001).

Proteases can be grouped into six major classes: aspartic, glutamic, serine, cysteine, threonine and metalloproteinases according to their catalytic mechanisms (Clark, 2001). Among these, metalloproteinases are the largest catalytic classes of proteases. The main characteristic of metalloproteinases is the requirement of zinc ions to polarize a water molecular for hydrolytic reaction (Visse, 2003). The three major classes of metalloproteinases are ADAMs (a disintegrin and metalloproteinase domain), ADAMTS (ADAMs with thrombospondin domain), and MMP (matrix metalloproteinase) (Clark, 2001).

ADAMs are a family of transmembrane and secreted metalloendopeptidase, which

1

can be characterized by a particular domain organization featuring a pro-domain, a

metalloprotease, a disintegrin, a cysteine-rich, an epidermal-growth factor like and a

transmembrane domain, as well as a C-terminal cytoplasmic tail (Brocker, 2009). They

are involved in cancer metastasis by cell adhesion and proteases activities (Karan et al.,

2003).

ADAMTS is a family of multidomain extracellular metalloproteinase

characterized by a disintegrin, a metalloprotease and a thrombospondin domain (Porter

et al., 2005). The substrates of ADAMTS include procollagens and von Willebrand

factor as well as cleavage of aggrecan, versican, brevican and neurocan, and this makes

ADAMTS the key remodeling enzymes of the extracellular matrix. They have been

demonstrated to have important roles in connective tissue organization, coagulation,

inflammation, arthritis, angiogenesis and cell migration (Apte, 2004).

Roles of MMPs in development and regeneration

MMPs, also called matrixins, are a group of secreted or membrane-anchored

metalloproteases. At least 25 different types of MMPs have been found in the

vertebrates. They can degrade most components of the extracellular matrix (ECM) and

further regulate the composition of the ECM (Nagase and Woessner, 1999). The

primary structure of MMPs in vertebrates consists of pro-peptide domain, catalytic

domain, hemopexin domain, GPI domain or transmembrane domain (Nagase and

Woessner, 1999). The removal of pro-peptide domain and zinc ion binding at catalytic

domain are essential for MMPs activation. The hemopexin domain, GPI domain and

transmembrane domain vary among different types of MMPs.

MMPs are transcriptionally regulated by growth factors, hormones, cytokines, and

cellular transformation (Ingraham et al., 2011; Ozeki et al., 2014, 2016). Also, MMP

proteins are activated by cleavage by other enzymes, and are inactivated by endogenous

inhibitors, such as α-macroglobulin and tissue inhibitors of metalloproteinases

(TIMPs)(Bai et al., 2005; Rodriguez-Calvo et al., 2015). Moreover, MMPs can modify

growth factors, receptors and adhesion molecules on the plasma membrane and

contribute to the regulation of cell proliferation and migration, respectively (Chang et

al., 2013; Nishihara et al., 2015; Wong et al., 2016). Therefore, tight regulation of

MMPs is essential for development and regeneration.
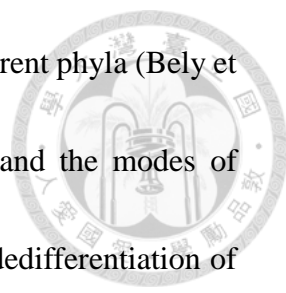
Extracellular matrix (ECM) is a collection of extracellular molecules, including

fibronectin, collagen and heparan sulfate, which is the main substrate of MMPs. ECM

provides structural and biochemical supports to the cells and plays important roles in

cell-cell adhesion, cell communication and signaling transduction (Nagase and

Woessner, 1999). In the development of different cell lineages, the composition of ECM

varies (Frantz et al., 2010). For example, the ECM in the basement membrane of skin

is mainly composed of collagen, laminin, entactin and heparan sulfate; however, the ECM in the blood vessel is composed of collagen, laminin, fibronectin and perlecan. Therefore, ECM is for development and regeneration due to the involvement of cell interaction, cell migration and tissue formation in these processes.

MMPs are involved in dealing with wound clearance and environment change (Yong, 2005; Zhang et al., 2009; Ingraham et al., 2011; Ma et al., 2014; Ozeki et al., 2014, 2015, 2016). Also, during the regenerative processes, the extracellular matrix around wounded sites changes violently. ECM remodeling must be well regulated. For example, in planarian, inhibiting *mmp1* caused a disruption of tissue and a decrease of cell death. After silencing of *mt-mmpA*, the planarian could not regenerate. Its tissue integrity was compromised and blastema formation was delayed. These results provide evidences of that MMPs regulate stem cells migration and proliferation during regeneration and body homeostasis in planarian (Isolani et al., 2013). Although MMPs were found involved in the regenerative processes, the mechanism and the regulation of MMPs are still unclear.

Regeneration
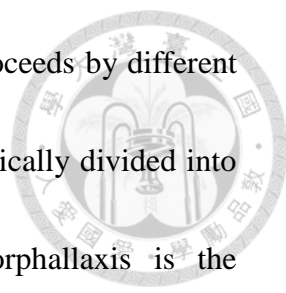
Regeneration is the process that restore the injured and lost body parts, organs, tissues and cells. It is one of the most amazing abilities in the animal Kingdom (Sanchez

4

Alvarado & Tsonis, 2006). This ability is broadly found among different phyla (Bely et al., 2014; Li et al., 2015). However, the regenerative capability and the modes of regeneration, such as the rearrangement of pre-existing tissue, the dedifferentiation of somatic cells, the transdifferentiation of cells around wounded sites and the migration and activation of somatic stem cells, are diverse (Agata et al., 2007; Agata & Umesono, 2008; Jopling et al., 2011; Li et al., 2015). More than one mode of regeneration can be observed in different tissues of same animal.
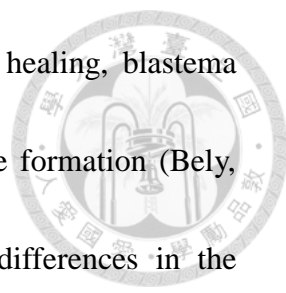
To understand the complicated mechanism of regeneration, some species with regenerative ability, such as hydra, planarian, teleost fish and amphibian, have been used as model animals to research regeneration. Although these models have regenerative ability, their capabilities of regeneration are remarkably different. Invertebrates like hydra and planarians have an amazing regenerative ability and can regenerate the whole body from a tiny body fragment. Vertebrates like amphibians and teleosts can only regenerate some lost body parts, such as limbs, heart or fins.

During the process of regeneration, the composition and morphology of cells and tissues change. *Xenopus* examplifies the general processes of vertebrate regeneration. After limb amputation, *Xenopus* goes through the following steps to regenerate the lost limb: wound healing, blastema formation, cell proliferation, tissue remodeling and finally the new limb formation (Suzuki et al., 2006).

5

Among the animals with regenerative ability, regeneration proceeds by different pathways or even by different types of cells. They have been classically divided into "morphallaxis" and "epimorphosis" (Agata et al., 2007). Morphallaxis is the regenerative process in which the rearrangement of pre-existing tissue makes the main contribution to complete regeneration. Hydra is the most well-known animal having this type of regeneration. On the other hand, epimorphosis is the regeneration type defined as "add-on" regeneration, which means that this type of regeneration involves a large amount of cell proliferation, resulting in blastema formation, without violent tissue rearrangement (Suzuki et al., 2006). The regeneration type of amphibians is typical for epimorphosis. However, no animal can be clearly classified into either one types of regeneration because all of them undergo tissue rearrangement and cell proliferation (Agata, 2007).

Among the model animals used for regeneration research, the invertebrates, such as hydra and planarian, shows a higher regenerative capability than that in the vertebrates, such as zebrafish and salamander. Also, the mechanism of regeneration in these invertebrate models is different from the vertebrates (Li et al., 2015). In previous researches, some annelids have been found with high regenerative ability (Zoran, 2010; Weidhase et al., 2014). Nonetheless, the regenerative mechanism of annelid is similar to that of vertebrate (Bely, 2014). The regenerative mechanism of annelid is mainly

6
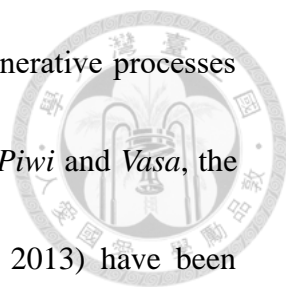
epimorphosis and its regenerative processes also include wound healing, blastema formation, cell proliferation, tissue remodeling and the new tissue formation (Bely, 2014). Thus, annelids might be a good model to resolve the differences in the regenerative mechanism across animal phyla. In addition, because of a variety of regenerative capacities are found in annelids, annelids might also be useful to clarify the evolution and the regulation of regeneration (Ferrier, 2012).

Aeolosoma viride in regeneration research

To further investigate the relationship between MMPs and regeneration and its evolution, a novel animal model from annelid phylum was used to fill the gap between planarian and vertebrates. *Aeolosoma viride* is a fresh water annelid with high regenerative ability. It has 12 segments and the entire body length is about 2-3 mm. The average lifespan of an individual is around 3 months, producing about 15 offspring (Falconi, 2006; Chen, 2016). It can complete anterior regeneration within 5 days (Tseng, 2016). It can be a good model for the research on regeneration due to its semi-transparency and asexual reproduction. These characteristics are beneficial to the various staining methods used in the related researches and mass cultivation in the lab.

Because *A. viride* is not yet a popular model for regeneration study, therefore, some technical difficulties exist for this non-model organisms. However, many systems

7

and tools have been developed in Dr. Chen's lab. Also, some regenerative processes

have also been characterized in previous researches. For example, *Piwi* and *Vasa*, the

markers of regenerative tissue, neoblast, in the planarian (Rink, 2013) have been

observed in the regenerating and reproducing tissue of *A. viride*. The expression of both

genes disappeared after exposed to the irradiation, suggesting these expressions are

stem cell specific. In addition, several pathways have been identify in the anterior

regeneration of *A. viride*, such as activin/TGF-β, Wnt, Toll and caspase, which will be

helpful to clarify the anterior regeneration in *A. viride*.

Aims

1. To identify whether MMPs are involved in the regeneration in A. viride.

2. To figure out what functions of MMPs in the regeneration are.

Material and method

Aeolosoma viride

Aeolosoma viride were cultured in the artificial spring water (ASW, 48 mg/L NaHCO$_3$, 24 mg/L CaSO$_4 \cdot$ 2H$_2$O, 30 mg/L MgSO$_4 \cdot$ 7H$_2$O and 2 mg/L KCl in ddH2O, pH=7.4) at 22 ± 1 ℃, and fed with ground oats every three days. Before experiments, worms were washed by tap water for 30 minutes and cultured in the clean ASW overnight for minimizing the oats in their gut. Then, they were synchronized, amputated just behind the swollen gut, to eliminate the differences of reproductive state. *A. viride* was amputated between fourth and fifth body segments, and, then, cultured in sterile ASW at 22 ℃ for *A. viride* to regenerate.
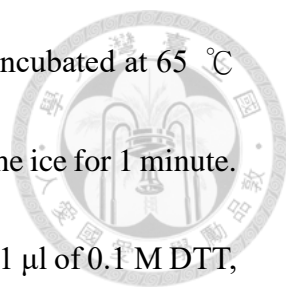
RNA extraction

Before extracting RNA, *A. viride* was washed three times with sterile ASW. Then, they were transferred into Trizol (Invitrogen, Carlsbad, CA) with minimal liquid and homogenized in Trizol. One fifth of Trizol's volume of chloroform was added into the homogenates and uniformly mixed with homogenates. Next, the sample was centrifuged at 14,000 rpm for 30 minutes at 4 ℃. The supernatant was transferred into another tube and uniformly mixed with the same volume of isopropanol. The mixture was keep in the -20 ℃ for 50 minutes to precipitate the RNA. After that, the sample

9

was again centrifuge at 14,000 rpm for 30 minutes at 4 ℃. After the supernatant removed, the RNA pellet was washed twice with 75 % ethanol and air-dried. Then, the pellet was re-dissolved into diethylpyrocarbonate-deionized water (DEPC-H_2O) and incubated at 50 ℃ for 15 minutes. The concentration of RNA was further measured by NanoDrop^{TM} ND-1000 (Thermo Scientific, Waltham, MA).

Reverse transcription

Extracted total RNA was reverse transcribed using SuperScript® III First-Strand Synthesis System (Invitrogen, Carlsbad, CA). Briefly, up to 5 μg of RNA was added with 1 μl of 50 μM oligo-(dT)$_{18}$ primer, 1 μl of 10 mM dNTP and DEPC-H_2O to a total volume of 10 μl. Then, the sample was incubated at 65 ℃ for 5 minutes to unwind the secondary structure of RNA and kept in the ice for 1 minute. Next, it was added with a mixture containing 2 μl of 10X RT buffer, 2 μl of 0.1 M DTT, 4 μl of 25 mM MgCl$_2$, 1 μl of RNase OUT^{TM} (Invitogen, Carlsbad, CA), 0.5 μl of SuperScript^{TM} III and 0.5 μl of DEPC-H_2O. Finally, the mixture was incubated at 50 ℃ for 50 minutes and the reaction was ceased through increasing temperature to 85 ℃ for 15 minutes. The protocol for Real-time quantitative polymerase chain reaction (qPCR) is similar to previous protocol but with some differences. The brief protocol is as follows: 600 ng of RNA was added with 1μl of 50 ng/μl random hexamer primer, 1 μl of 10 mM dNTP

10

and DEPC-H$_2$O to a total volume of 5 μl. Second, the sample was incubated at 65 ℃

for 5 minutes to unwind the secondary structure of RNA and kept in the ice for 1 minute.

Third, it was added with a mixture containing 1 μl of 10X RT buffer, 1 μl of 0.1 M DTT,

2 μl of 25 mM MgCl$_2$, 0.5 μl of RNase OUT^{TM}, 0.25 μl of SuperScript^{TM} III and 0.25

μl of DEPC-H$_2$O. Fourth, after incubating at 25 ℃ for 10 minutes, the mixture was

incubated at 50 ℃ for 50 minutes. Fifth, the reaction was ceased through increasing

temperature to 85 ℃ for 15 minutes. Finally, the sample was added with 1 U RNase

H (Invitogen, Carlsbad, CA) and incubating at 37 ℃ for 20 minutes to exclude the

effects of RNA during qPCR.

Gene cloning

Specific primers were designed according to the partial sequences obtained from

Next Generation Sequencing (NGS) data from Chen's lab. The sequences were

confirmed through polymerase chain reaction (PCR) and further extended by 3' rapid

amplification of cDNA ends (3'RACE) and 5'RACE methods.

Real-time quantitative PCR

After the cDNA for qPCR prepared as mentioned previously, gene expression

levels were detected by specific primers, SYBR® Green Master Mix (Bio-Rad,

11
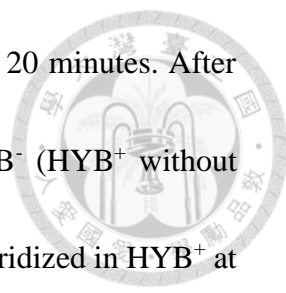
Hercules, CA) and iCycler iQ Realtime detection system (Bio-Rad, Hercules, CA).

In situ hybridization
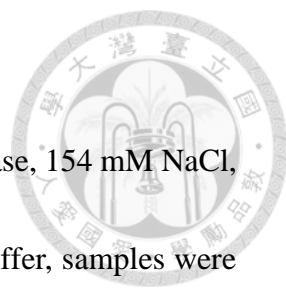
Targeting sequences were amplified through PCR by specific primers and inserted into yT&A vector (Yeastern Biotech, Taiwan). Vectors with inserted sequence were selected and used for *in vitro* transcription by using T7 polymerase (Promega, Madison, WI) and DIG-labeled rNTP (Ambion, Foster, CA). Then, after DNA templates were digested by added RNase free DNase I (Promega, Madison, WI), the ssRNA products were precipitated with 1 μl of 0.5 M EDTA (pH 8.0), 2.5 μl of LiCl and 75.5 μl of ethanol at -20 ℃ for 50 minutes. After that, the extracting protocol of probes is identical to the RNA extracting protocol described earlier. Finally, the DIG-labeled probes were dissolved in HYB$^+$ buffer (50 % formamide, 5X saline sodium citrate (SSC), 9.2 mM citric acid, 50 μg/ml heparin, 0.5 mg/ml yeast tRNA (Sigma, St. Louis, MO) and 0.1 % Tween-20 in DEPC-H$_2$O).

Before *in situ* hybridization, collected samples were washed by sterile ASW and fixed in 4 % paraformaldehyde (PFA) at 4 ℃ overnight. Next, after washed by phosphate buffered saline with 0.1 % Tween-20 (PBST, pH 7.4) 5 times, samples were gradually transferred into methanol and maintained at -20 ℃ overnight. In the next day, samples were gradually transferred into PBST and treated with 10 mg/ml protease

12

K for 10 minutes. Then, the samples were refixed in 4 % PFA for 20 minutes. After washed by PBST 5 times, the samples were transferred into HYB$^-$ (HYB$^+$ without heparin and yeast tRNA) at 65 ℃ for 1 hour. Samples were prehybridized in HYB$^+$ at 65 ℃ for 1 hour and then hybridized at 65 ℃ overnight in HYB$^+$ with 1 ng/μl DIG-labed RNA probe. After hybridization, samples were briefly washed by HYB$^-$ and then gradually changed to 2X SSCTw (SSC with 0.1 % Tween-20). Then, after incubated in 2X SSCTw at 65 ℃ for 5 minutes, samples were washed by 0.2 X SSCTw at 65 ℃ for 15 minutes twice. Next, samples were gradually transferred into PBST at 25 ℃ and performed blocking with blocking buffer (5 % bovine serum albumin (BSA, Sigma, St. Louis, MO) in PBST) for 2 hours. After blocking, the samples were transferred into blocking buffer with anti-DIG antibody conjugated with AP (1:10000 diluted, Roche, Basel, Switzerland) at 4 ℃ overnight. Prior to staining, samples were washed by PBST 5 times at 25 ℃ for 5 minutes and transferred into staining buffer (100 mM Tris-HCl pH 9.5, 50 mM MgCl$_2$ and 100 mM NaCl in 0.1 % Tween-20) for 3 times. Then, samples were immersed in the staining buffer with NBT and BCIP without shacking and light. The stained samples were washed by PBST 5 times and gradually dehydrated with methanol. For microscopy, samples were gradually rehydrate with PBST and mounted with Fluoromount-G™ (eBioscience, San Diego, CA)

13

Zymograph

Protein samples were extracted by RIPA buffer (65 mM Tris-base, 154 mM NaCl, 1 mM EDTA, 1 % SDS, pH 7.4). After homogenized with RIPA buffer, samples were centrifuged at 13,000 rpm for 15 minutes at 4 ℃. The supernatant was transferred to a new tube for later use. Protein concentration was determined by Bradford reagent (Sigma, St. Louis, MO). Next, 20 μg protein sample was mixed with 2X sampling buffer (4% SDS, 20% Glycerol, 0.12M Tris, 1 mM Orange G, pH 6.8) and loaded into a polyacrylamide gel with 1 % gelatin. After proteins were separated by sodium dodecyl sulfate polyacrylamide gel electrophoresis (SDS-PAGE) for 3 hours at 4 ℃, the gel were soaked into 2.5 % TritonX-100 in PBST four 30 minutes to replace SDS and renature the MMPs. Then, the gel was immersed in working buffer (50 mM Tris-HCl, 25 mM $CaCl_2$, 5 μM $ZnSO_4$, pH 7.4) for 30 minutes at 25 ℃. Finally, gel was stained by Brilliant Blue R 250 (Sigma, St. Louis, MO).

Statistic

All the experiments were representative of three replications. The results were showed as means $\pm$ standard deviation. One-way ANOVA were performed to determine the statistical significant levels.

Results
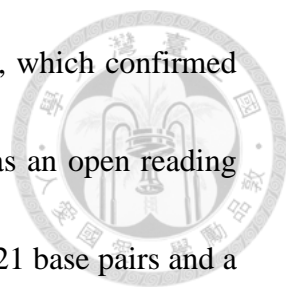
Sequencing of *Avi-mmp14*, *Avi-mmp17*, *Avi-mmp21* and a MMP-like gene, *Avi-mmp-like gene*

According to the sequences in the NGS data of regenerating *A. viride*, the primers were designed to clone the mRNA sequences of *mmps*. Three *mmps* have been cloned and named as *Avi-mmp14*, *Avi-mmp17* and *Avi-mmp21*, respectively. *Avi-mmp14* has an open reading frame of 1698 base pairs, encoding 566 amino acids, a 5' untranslated region (UTR) of 145 base pairs and a 3' UTR of 466 base pairs (Figure 1A and 1B). According to protein domain prediction from Simple Modular Architecture Research Tool (SMART) and Center for Biological Sequence Analysis (CBS), a signal peptide can be found at the first 30 amino acid from the N-terminal. The substrate binding domain at 34-101 amino acid, zinc-dependent metalloproteinase catalytic domain (ZnMc) at 126-287 amino acid and hemopexin-like repeat at 333-377, 379-427, 429-477 and 479-521 amino acid can be observed in the protein sequence of *Avi*-MMP14. (Figure 1C) These three domains are common in the MMPs. Also, a transmembrane domain can be observed at 530-560 amino acid in the protein sequence showed as blue rectangle in Figure 1C. The open reading frame of *Avi-mmp17* is 1434 base pairs, encoding 478 amino acids, with a 5' UTR of 255 base pairs and a 3' UTR of 885 base pairs (Figure 1D and 1E). The protein domain prediction showed a substrate binding
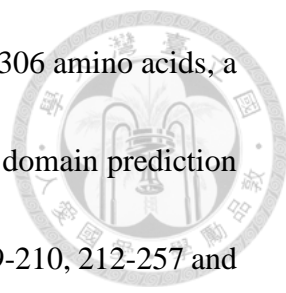
15

domain and a ZnMc domain at 140-192 and 227-386, respectively, which confirmed

that *Avi-mmp17* also belongs to MMPs (Figure 1F). *Avi-mmp21* has an open reading

frame of 2349 base pairs, encoding 783 amino acids, a 5' UTR of 121 base pairs and a

3' UTR of 802 base pairs (Figure 1G and 1H). By protein prediction, the signal peptide

at first 47 amino acid, ZnMc domain at 322-493 amino acid and hemopexin-like repeats

domains at 511-558, 560-612 and 623-671 amino acid can be observed in protein

sequence of *Avi*-MMP21 (Figure 1I).

To further confirm the sequence that had been cloned, *Avi*-MMPs sequences were

used to draw phylogenetic trees with other published sequences of MMPs in the

National Center for Biotechnology Information (NCBI) database. The full-length

phylogenetic tree of MMPs showed that both of MMP14 and MMP17 have two groups,

invertebrate and vertebrate. *Avi-MMP21* is grouped with MMP21. *Avi*-MMP14 is

grouped with MMP14 of invertebrate. However, *Avi*-MMP17 is grouped with Zinc

Metalloproteinase of *C. elegans* (Figure 2A). In the catalytic domain phylogenetic tree

of MMPs, it showed that MMPs can be roughly divided into two groups, membrane

type and secreted form. *Avi*-MMP17 is grouped with other MMP17 of invertebrate. *Avi*-

MMP21 is grouped with MMP21. And *Avi*-MMP14 is grouped with other membrane

type MMPs (Figure 2B). These results can further confirm the identity of *Avi*-MMPs.

In this study, one more mmp-like gene was also found and cloned. *Avi-mmp-like*

16

gene has a partial cloned sequence about 1078 base pairs, encoding 306 amino acids, a

3' UTR of 106 base pairs (Figure 3A and 3B). According to protein domain prediction

from SMART and CBS, four hemopexin-like repeats at 124-167, 169-210, 212-257 and

259-302 amino acid can be observed in the protein sequence of *Avi*-MMP-like gene.

(Figure 3C) These domains are common in the MMPs. However, it lacks the most

important domain, zinc-dependent metalloproteinase catalytic domain. Therefore, I

named it as *Avi-mmp-like* gene.

The quantification gene expression of *mmps* in *A. viride* during anterior regeneration

To test the involvement of *Aeolosoma's mmps* into regeneration, real-time

quantitative PCR were used to detect the mRNA expression level of *Aeolosoma's mmps*.

The blastema of various regenerating stages were collected to detect the mRNA

expression level. As seen in Figure 4, the gene expression of *Avi-mmp14* had no

significant changes during the regeneration. In contrast, the gene expression of *Avi-mmp17* at blastema upregulated after 6 hpa and reached highest level at 12 hpa, which

was 8 folds increase from the intact head. Then, the expression level decreased slowly

after 48 hpa through the regeneration. Expression of *Avi-mmp21* was similar to that of

Avi-mmp17, increasing after 6 hpa, reaching the highest level at 12 hpa, and decreasing

17

to the normal level after 72 hpa. These results suggested that *Avi-mmp17* and *Avi-mmp21* might be involved in the early stage of anterior regeneration. In the *Avi-mmp-like gene*, the gene expression at blastema decreased before 24 hpa and upregulated after 48 hpa. Then, the expression remained high, 4-fold to intact head, after 96 hpa until the regeneration finished. This result suggested that *Avi-mmp-like gene* might be involved in the late stage of anterior regeneration.
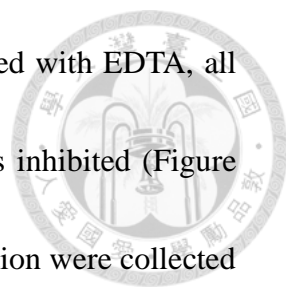
Gene expression of *Avi-mmps* at the blastema during anterior regeneration

To identify the location of *Avi-mmps* expression during regeneration, RNA probes were designed to detect the mRNA. The primers designed for making RNA probes showed at Table 3. For high specificity, the RNA probes were designed about 700-800 nucleotides with sequences including UTR and open reading frame (OPF). *In situ* hybridization of *Avi-mmp14*, *Avi-mmp17* or *Avi-mmp21* were performed on intact and regenerating samples (Figure 5, 6 and 7). During regeneration, staining for *Avi-mmp14* made no significant changes, which was widely distributed in the whole body, including blastema in various regenerative stages (Figure 5B). These data were consistent with the qPCR results as shown in Figure 4. For *Avi-mmp17*, staining also appeared at the blastema after 12 hpa. The signals reached the highest level around 48 hpa and

18

decreased back to the normal level at 120 hpa (Figure 6B). Staining for *Avi-mmp21*

could be observed in the blastema after 6 hpa the signal reached the highest level at 24

hpa and 48 hpa, slowly decreased after 72 hpa during the anterior regeneration and fell

back to normal level after 96 hpa (Figure 7B).

The enzymatic activity of *Avi*-MMPs at the early stage of anterior regeneration
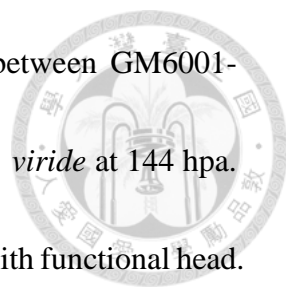
To test if Avi-MMPs are activated during the regenerative processes. SDS-PAGE

gelatin zymograph was used as a tool to detect the enzymatic activity of MMPs during

regeneration in *A. viride*. The zymograph showed three clear bands in the gel after

stained with commassie blue which means that there are at least three enzymes of

different molecular weights, 80 KD, 55 KD and 45 KD, with gelatinolytic activity in

the *A. viride* crude protein extract (Figure 8A). In previous *Avi*-MMPs protein

molecular weight prediction, *Avi*-MMP14 is about 63 KD, *Avi*-MMP17 is about 53.22

KD and *Avi*-MP21 is about 85.75 KD. After signal peptide removal, *Avi*-MMP14 is

about 59.64 KD and *Avi*-MP21 is about 80.41 KD. Thus, the three active enzyme found

in the gelatin zymograph might be the three *Avi*-MMPs that have been cloned. To

further   confirm   these   enzymes   belonging   to   metalloproteinases,

Ethylenediaminetetraacetic acid (EDTA) was used to chelate the bivalent cations, such

19

as zinc ion, to inhibit the enzymatic activity of MMPs. After treated with EDTA, all

bands became reduced, suggesting that the enzymatic activity was inhibited (Figure

8A). Furthermore, the blastemas of early stage of anterior regeneration were collected

to do the zymograph. The zymograph showed the activity of all the three MMPs had a

peak at 24 hpa, and the activity decreased back to normal level at 48 hpa (Figure 8B).

In the statistical analysis, the activities of three MMPs at 48 hpa were significantly

higher, up to two folds of the activity about intact head (Figure 8C). These results

suggested that three MMPs are active in the early stage of anterior regeneration.

Inhibition of the activity of MMPs causing impaired regeneration

To further test the participation of MMPs in regeneration, a broad-spectrum matrix

metalloproteinase inhibitor, GM6001, was used. GM6001, a hydroxamic acid, can form

a bidentate complex with the zinc at the active site of MMPs. Thus, it can reversibly

inhibit the enzymatic activity of MMPs. After treated with different concentration of

GM6001, the success rate of regeneration at 144 hpa significantly decreased with a

concentration-dependent manner. When treated with 200 μM GM6001, the success rate

of regeneration at 144 hpa significantly decreased to about 20 % (Figure 9A). Thus,

this concentration was selected for further inhibitory studies on regeneration. To figure

out the function of MMPs in the regeneration, the amputated *A. viride* at 144 hpa were

20

collected to take a closer look on their morphology differences between GM6001-treating groups and control groups. The photos are the amputated *A. viride* at 144 hpa. In the group without GM6001, the anterior regeneration completed with functional head. However, in the group treated with 200 μM of GM6001, most of the regeneration failed. Some of the worms were stuck at wound healing stage, which showed little or no blastema. And, others became cysts and lay dormant until they die (Figure 9B). To further figure out the whether the function of MMPs on the regeneration is time-dependent, 200 μM GM6001 was used to treat the worms at different time periods of regeneration. The results showed that GM6001 treatment before 24 hpa had strong inhibitory effect on regeneration. When treated with GM6001 at 0-6 hpa and 6-12 hpa, the success rate of regeneration was about 50 %. Surprisingly, the most effective inhibition was when treated with GM6001 at 0-12 hpa, yielding a success rate of about 10-20 % (Figure 9D). When treated at 0-6 hpa and 12-24 hpa, the success rate of regeneration was high, suggesting a partial inhibition due to missing the critical period for MMPs' activities in regeneration.

The model of MMPs involved in the anterior regeneration in *A. viride*

In the previous studies done in our lab, the regenerative processes of the anterior regeneration in A. viride had been observed. It showed that the wound healing is

21

completed at 6 hpa. The blastema can be observed after 24 hpa. And the mouth opening appeared at 53 hpa. Finally, the anterior regeneration completed at 120 hpa (Figure 10). In this thesis, it was shown that at least three MMPs were involved in the anterior regeneration of A. viride. Two of MMPs, *Avi*-MMP17 and *Avi*-MMP21, might play crucial roles in the early stage of anterior regeneration. After their activities were inhibited by MMP inhibitor, GM6001, the regeneration failed. And, the other one MMP, *Avi*-MMP-like gene, might be involved in the late stage of anterior regeneration (Figure 10).

Discussion
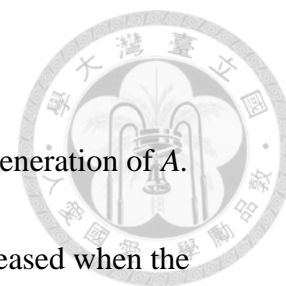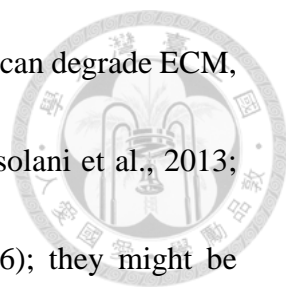
In this study, MMPs were found to be required for anterior regeneration of *A. viride* as the regenerative successful rate at 6 dpa significantly decreased when the enzyme activity of MMPs was inhibited. In addition, the gene expression and enzymatic activity of MMPs appeared in blastema. These findings suggest that MMPs should play a crucial role in the anterior regeneration of *A. viride*.

Four MMPs have been cloned from *A. viride* and sequenced. The number of MMP types is similar to that in planarian (4) (Isolani et al., 2013) and *Drosophila* (2) (Pearson et al., 2016). However, it is much lower than that in vertebrate, such as *Xenopus* (33) (Fu et al., 2009), human (23) and mouse (23) (Jackson et al., 2010). Why is there such a big difference between vertebrates and invertebrates? There is no obvious explanation yet.
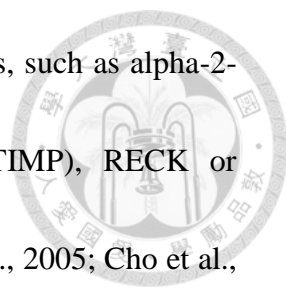
Due to their different functions and domain organizations, MMPs can be simply divided into two groups, MT-MMPs and MMPs (Nagase and Woessner, 1999). In MT-MMPs, the transmembrane domain usually exists near the C-terminus (Nagase and Woessner, 1999). However, *Avi*-MT-MMPs have predicted transmembrane domain near the N-terminus, which is similar to MT-MMPs found in planarian (Isolani et al., 2013).

The qPCR results showed that the expression of *Avi-mmp14* made no significant change during regeneration. However, *Avi-mmp17* and *Avi-mmp21* are significantly

23

upregulated in the early stage of anterior regeneration. Since MMPs can degrade ECM,

transduce signals and release growth factors (Chang et al., 2013; Isolani et al., 2013;

Ma et al., 2014; Wang & Page-McCaw, 2014; Wong et al., 2016); they might be

involved in *A. viride* regeneration processes. Wound closure, somatic cells

dedifferentiation and stem cell proliferation and migration are important events in the

early stage of regeneration, but remodeling of differentiated tissues, apoptosis of

redundant cells and promoting cell differentiation are the major events existed at late

stage of regeneration (Suzuki et al., 2006; Rink, 2013). Therefore, since *Avi-mmp17*

and *Avi-mmp21* were found upregulated in early stages of the regeneration, they may

be involved in wound closure and blastema formation. In the phylogenetic tree, *Avi-*

MMP14 is grouped with MMP14. In previous study, the activity of MMP14 can be

regulated through internalization in clathrin-coated vesicles (Fanjul-Fernandez et al.,

2010). Although the expression of *Avi-mmp14* had no significant change during

regeneration, it might be involved in the regeneration by externalization and increase

the enzyme activity.

In SDS-PAGE gelatin zymograph, three active MMPs have been found. And, their

enzymatic activity reached maximum at 24 hpa and sharply decreased back to normal

level at 48 hpa during the early stage of regeneration. These results showed the activity

of MMPs is well regulated during the regeneration. The sharp decreasing of the

24

enzymatic activities might be caused by the native MMP inhibitors, such as alpha-2-macroglobulin (A2M), tissue inhibitor of metalloproteinase (TIMP), RECK or extracellular matrix protection factors (Junseo et al., 2001; Bai et al., 2005; Cho et al., 2014; Rodriguez-Calvo et al., 2015). A2M has been found to inhibit active MMPs through trapping the active form of MMPs (Rodriguez-Calvo et al., 2015). TIMPs are a family of endogenous MMPs inhibitors, which can bind with hemopexin-like domain of pro-MMPs to inhibit their activities (Murphy, 2011). In this study, those mentioned MMP inhibitors have not been identified in *A. viride*. Therefore, a synthesized MMP inhibitor, GM6001 was used to test the function of MMPs in the regeneration.

After treatment with GM6001 the success rate of regeneration significantly decreased in *A. viride*. In zebrafish, GM6001 treatment causes failure of tail regeneration (Bai et al., 2005). These suggest that the activity of MMPs is crucial for regeneration. When treated with GM6001 at different period of anterior regeneration, the maximum inhibition on regeneration appeared in 0-12 hpa. This result matches the timing of maximum gene expression of *Avi-mmp17* and *Avi-mmp21*. Therefore, these results suggest that both *Avi-mmp17* and *Avi-mmp21* are involved at the early stage of the anterior regeneration in *A. viride*, which should include wound closure, growth factor release, cell dedifferentiation, stem cells maintenance and cells migration. (Armstrong & Jude, 2002; Satoh et al., 2011; Isolani et al., 2013; Andries et al., 2016;

25

J. Wu et al., 2016). When enzymatic activities of those MMPs are inhibited, those

regenerative processes are affected and results in decreasing the regeneration successful

rate. Some of MMPs act as activator of other MMPs, such as MMP14 (Lee et al., 2013).
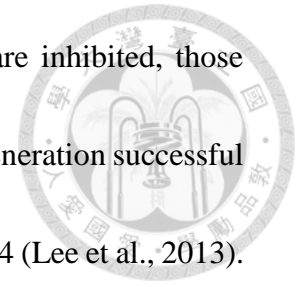
Thus, it might form a activating cascade to form active MMPs. In the inhibition data,

treatment with GM6001 at the 0-6 hpa and 12-24 hpa had partial inhibition effect, which

might be caused by initiating the activating cascade.

In the study, MMPs were found to be essential at early stage of the anterior

regeneration. However, how these enzymes are regulated remains unknown. In

previous studies, Wnt signaling pathway has been found in upstream of some MMPs

(Ingraham et al., 2011; Wang & Page-McCaw, 2014 ; Ozeki et al., 2014, 2016). Also,

Wnt signaling pathway upregulates at the wound site to promote cell proliferation,

tissue polarity and apoptosis (Petersen & Reddien, 2008; Chera et al., 2009; Jameson

et al., 2012; Wu et al., 2014; Ozhan & Weidinger, 2015). Thus, at the early stage of the

anterior regeneration, Wnt signaling pathway might be at upstream of both *Avi*-MMP17

and *Avi*-MMP21. In addition, fibrinolytic enzymes are a group of enzymes with

anticoagulation activity (Kim, 2014). In human, some fibrinolytic enzymes, such as

plasminogen activator and plasmin can regulate MMPs activity (Lijnen, 2002; Chang

et al., 2011; Munakata et al., 2015). Since two fibrinolytic enzymes also showed high

enzymatic activity and their gene expressions upregulate at early stage of anterior

26

regeneration in *A. viride* (Tseng and Chen, 2014), fibrinolytic enzyme might regulate the MMPs during the anterior regeneration. More, Extracellular matrix metalloproteinase inducer (EMMPRIN), a transmembrane glycoprotein expressed on epithelial cells (Hasaneen et al., 2016; Wu et al., 2016), can induce MMPs in neighboring stromal cells through direct epithelial-stromal interactions. These activators might regulate MMPs during the regeneration. Thus, the regulation of MMPs during the regeneration in *A. viride* needs to be studies in the future.

27
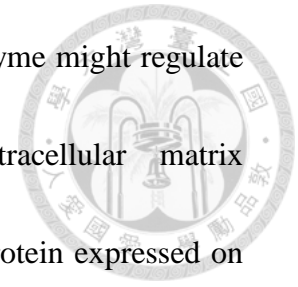
Reference

Agata, K., Saito, Y., & Nakajima, E. (2007). Unifying principles of regeneration I: Epimorphosis versus morphallaxis. Dev Growth Differ, 49(2), 73-78.

Agata, K., & Umesono, Y. (2008). Brain regeneration from pluripotent stem cells in planarian. Philos Trans R Soc Lond B Biol Sci, 363(1500), 2071-2078.

Andries, L., Van Hove, I., Moons, L., & De Groef, L. (2016). Matrix Metalloproteinases during Axonal Regeneration, a Multifactorial Role from Start to Finish. Mol Neurobiol.

Apte SS. (2004). A disintegrin-like and metalloprotease (reprolysin type) with thrombospondin type 1 motifs: the ADAMTS family. Int J Biochem Cell Biol. 36(6), 981-5.

Armstrong, D. G., & Jude, E. B. (2002). The Role of Matrix Metalloproteinases in Wound Healing. Journal of the American Podiatric Medical Association, 92(1), 12-18.

Bai, S. Thummel, R. Godwin, A. R. Nagase, H. Itoh, Y. Li, L. Evans, R. McDermott, J. Seiki, M. Sarras, M. P., Jr. (2005). Matrix metalloproteinase expression and function during fin regeneration in zebrafish: analysis of MT1-MMP, MMP2 and TIMP2. Matrix Biol, 24(4), 247-260.

Bely, A. E. (2014). Early events in annelid regeneration: a cellular perspective. Integr

Comp Biol, 54(4), 688-699.

Bely, A. E., Zattara, E. E., & Sikes, J. M. (2014). Regeneration in spiralians: evolutionary patterns and developmental processes. Int J Dev Biol, 58(6-8), 623-634.

Brocker CN, Vasiliou V, Nebert DW. (2009). Evolutionary divergence and functions of the ADAM and ADAMTS gene families. Hum Genomics., 4(1),43-55.

Chang, C. H. Huang, Y. L. Shyu, M. K. Chen, S. U. Lin, C. H. Ju, T. K. Lu, J. Lee, H. (2013). Sphingosine-1-phosphate induces VEGF-C expression through a MMP-2/FGF-1/FGFR-1-dependent pathway in endothelial cells *in vitro*. Acta Pharmacol Sin, 34(3), 360-366.

Chang, Y. M. Shih, Y. T. Chen, Y. S. Liu, C. L. Fang, W. K. Tsai, C. H. Tsai, F. J. Kuo, W. W. Lai, T. Y. Huang, C. Y. (2011). Schwann Cell Migration Induced by Earthworm Extract via Activation of PAs and MMP2/9 Mediated through ERK1/2 and p38. Evid Based Complement Alternat Med, 2011, 395458.

Chera, S. Ghila, L. Dobretz, K. Wenger, Y. Bauer, C. Buzgariu, W. Martinou, J. C. Galliot, B. (2009). Apoptotic cells provide an unexpected source of Wnt3 signaling to drive hydra head regeneration. Dev Cell, 17(2), 279-289.

Cho, E., Chmielewski, S., Nolt, J., Klunk, J., Youngwirth, J., Palumbo, A., Maugle, T., Lukashova, L., Belogorodsky, D., Holmes, T., Althauser, S., Pinkney, N., Selim,

29
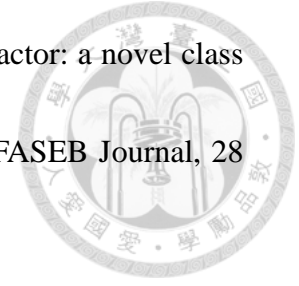
A., D'Angelo, M. (2014). Extracellular matrix protection factor: a novel class of post-traumatic osteoarthritis therapeutic (922.11). The FASEB Journal, 28 (1 Supplement).

Chen, C.F. (2016). The Roles of Telomerase in Regeneration during Aging and the Telomeric DNA Sequence Identification in *Aeolosoma viride* (1051.2). The FASEB Journal, 30 (1 Supplement)

Christian Frantz, K. M. S. a. V. M. W. (2010). The extracellular matrix at a glance. Journal of Cell Science, 123, 4195-4200.

Clark, I. M. (2001). Matrix metalloproteinase protocols. 151.

Fanjul-Fernandez, M., Folgueras, A. R., Cabrera, S., & Lopez-Otin, C. (2010). Matrix metalloproteinases: evolution, gene regulation and functional analysis in mouse models. Biochim Biophys Acta, 1803(1), 3-19.

Falconi R., Renzulli T., Zaccanti F. (2006). Survival and reproduction in *Aeolosoma viride* (Annelida, Aphanoneura). Hydrobiologia 564, 95–99.

Ferrier, D. E. (2012). Evolutionary crossroads in developmental biology: annelids. Development, 139(15), 2643-2653.

Fu, L., Das, B., Mathew, S., & Shi, Y. B. (2009). Genome-wide identification of *Xenopus* matrix metalloproteinases: conservation and unique duplications in amphibians. BMC Genomics, 10, 81.

Hasaneen, N. A., Cao, J., Pulkoski-Gross, A., Zucker, S., & Foda, H. D. (2016). Extracellular Matrix Metalloproteinase Inducer (EMMPRIN) promotes lung fibroblast proliferation, survival and differentiation to myofibroblasts. Respir Res, 17(1), 17.

Ingraham, C. A., Park, G. C., Makarenkova, H. P., & Crossin, K. L. (2011). Matrix metalloproteinase (MMP)-9 induced by Wnt signaling increases the proliferation and migration of embryonic neural stem cells at low O_2 levels. J Biol Chem, 286(20), 17649-17657.

Isolani, M. E., Abril, J. F., Salo, E., Deri, P., Bianucci, A. M., & Batistoni, R. (2013). Planarians as a model to assess *in vivo* the role of matrix metalloproteinase genes during homeostasis and regeneration. PLoS One, 8(2), e55649.

Jackson BC, N. D., Vasiliou V. (2010). Update of human and mouse matrix metalloproteinase families. Hum Genomics., 4(3), 194-201.

Jameson, S. A., Lin, Y. T., & Capel, B. (2012). Testis development requires the repression of Wnt4 by Fgf signaling. Dev Biol, 370(1), 24-32.

Jopling, C., Boue, S., & Izpisua Belmonte, J. C. (2011). Dedifferentiation, transdifferentiation and reprogramming: three routes to regeneration. Nat Rev Mol Cell Biol, 12(2), 79-89. doi:10.1038/nrm3043

Junseo Oh, R. T., Shunya Kondo, Akira Mizoguchi, Eijiro Adachi, Regina M. Sasahara,
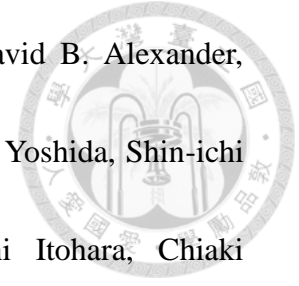
Sachiko Nishimura, Yukio Imamura, Hitoshi Kitayama, David B. Alexander, Chizuka Ide, Thomas P. Horan, Tsutomu Arakawa, Hisahito Yoshida, Shin-ichi Nishikawa, Yoshifumi Itoh, Motoharu Seiki, Shigeyoshi Itohara, Chiaki Takahashi, Makoto Noda. (2001). The Membrane-Anchored MMP Inhibitor RECK Is a Key Regulator of Extracellular Matrix Integrity and Angiogenesis. Cell, 107(6), 789-800.

Karan D, Lin FC, Bryan M, Ringel J, Moniaux N, Lin MF, Batra SK. (2003). Expression of ADAMs (a disintegrin and metalloproteases) and TIMP-3 (tissue inhibitor of metalloproteinase-3) in human prostatic adenocarcinomas. Int J Oncol., 23(5), 1365-71.

Kim D. W., Choi J. H., Park S. E., Kim S., Sapkota K., Kim S. J. (2014). Purification and characterization of a fibrinolytic enzyme from *Petasites japonicas*. Int J Biol Macromol. 72, 1159-67.

Lee, H., Chang, K. W., Yang, H. Y., Lin, P. W., Chen, S. U., & Huang, Y. L. (2013). MT1-MMP regulates MMP-2 expression and angiogenesis-related functions in human umbilical vein endothelial cells. Biochem Biophys Res Commun, 437(2), 232-238.

Li, Q., Yang, H., & Zhong, T. P. (2015). Regeneration across metazoan phylogeny: lessons from model organisms. J Genet Genomics, 42(2), 57-70.

Lijnen HR. (2002). Matrix Metalloproteinases and Cellular Fibrinolytic Activity. Biochemistry (Mosc), 67(1), 92-98.

Ma, J., Tang, X., Wong, P., Jacobs, B., Borden, E. C., & Bedogni, B. (2014). Noncanonical activation of Notch1 protein by membrane type 1 matrix metalloproteinase (MT1-MMP) controls melanoma cell proliferation. J Biol Chem, 289(12), 8442-8449.

Munakata S, Tashiro Y, Nishida C, Sato A, Komiyama H, Shimazu H, Dhahri D, Salama Y, Eiamboonsert S, Takeda K, Yagita H, Tsuda Y, Okada Y, Nakauchi H, Sakamoto K, Heissig B, Hattori K. (2015). Inhibition of plasmin protects against colitis in mice by suppressing matrix metalloproteinase 9-mediated cytokine release from myeloid cells. Gastroenterology, 148(3), 565-578 e564.

Murphy, G. (2011). Tissue inhibitors of metalloproteinases. Genome Biology, 12.

Neitzel, J. J. (2010). Enzyme Catalysis: The Serine Proteases. Nature Education 3(9), 21.

Nishihara T, Remacle AG, Angert M, Shubayev I, Shiryaev SA, Liu H3, Dolkas J, Chernov AV, Strongin AY, Shubayev VI. (2015). Matrix metalloproteinase-14 both sheds cell surface neuronal glial antigen 2 (NG2) proteoglycan on macrophages and governs the response to peripheral nerve injury. J Biol Chem, 290(6), 3693-3707.

Ozeki, N. Hase, N. Hiyama, T. Yamaguchi, H. Kawai, R. Kondo, A. Nakata, K. Mogi, M (2014). IL-1beta-induced, matrix metalloproteinase-3-regulated proliferation of embryonic stem cell-derived odontoblastic cells is mediated by the Wnt5 signaling pathway. Exp Cell Res, 328(1), 69-86.
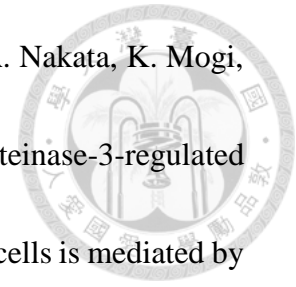
Ozeki, N. Kawai, R. Hase, N. Hiyama, T. Yamaguchi, H. Kondo, A. Nakata, K. Mogi, M. (2015). Alpha2 integrin, extracellular matrix metalloproteinase inducer, and matrix metalloproteinase-3 act sequentially to induce differentiation of mouse embryonic stem cells into odontoblast-like cells. Exp Cell Res, 331(1), 21-37.

Ozeki, N. Mogi, M. Hase, N. Hiyama, T. Yamaguchi, H. Kawai, R. Kondo, A. Nakata, K. (2016). Wnt16 Signaling Is Required for IL-1beta-Induced Matrix Metalloproteinase-13-Regulated Proliferation of Human Stem Cell-Derived Osteoblastic Cells. Int J Mol Sci, 17(2).

Ozhan, G., & Weidinger, G. (2015). Wnt/beta-catenin signaling in heart regeneration. Cell Regen (Lond), 4(1), 3.

Pearson, J. R. Zurita, F. Tomas-Gallardo, L. Diaz-Torres, A. Diaz de la Loza Mdel, C. Franze, K. Martin-Bermudo, M. D. Gonzalez-Reyes, A. (2016). ECM-Regulator timp is Required for Stem Cell Niche Organization and Cyst Production in the Drosophila Ovary. PLoS Genet, 12(1), e1005763.

Petersen, C. P., & Reddien, P. W. (2008). Smed-betacatenin-1 is required for

anteroposterior blastema polarity in planarian regeneration. Science, 319(5861), 327-330.
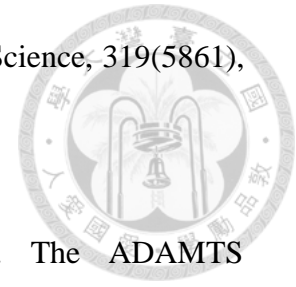
Porter S, Clark IM, Kevorkian L, Edwards DR. (2005). The ADAMTS metalloproteinases. Biochem J. 386(Pt 1), 15-27.

Rink, J. C. (2013). Stem cell systems and regeneration in planarian. Dev Genes Evol, 223(1-2), 67-84.

Rodríguez-Calvo R, Ferrán B, Alonso J, Martí-Pàmies I, Aguiló S, Calvayrac O, Rodríguez C, Martínez-González J. (2015). NR4A receptors up-regulate the antiproteinase alpha-2 macroglobulin (A2M) and modulate MMP-2 and MMP-9 in vascular smooth muscle cells. Thromb Haemost, 113(6), 1323-1334.

Sanchez Alvarado, A., & Tsonis, P. A. (2006). Bridging the regeneration gap: genetic insights from diverse animal models. Nat Rev Genet, 7(11), 873-884.

Satoh, A., makanae, A., Hirata, A., & Satou, Y. (2011). Blastema induction in aneurogenic state and Prrx-1 regulation by MMPs and FGFs in *Ambystoma mexicanum* limb regeneration. Dev Biol, 355(2), 263-274.

Suzuki, M., Yakushiji, N., Nakada, Y., Satoh, A., Ide, H., & Tamura, K. (2006). Limb regeneration in *Xenopus laevis* froglet. ScientificWorldJournal, 6 Suppl 1, 26-37.

Tseng, T. L., Chen J. H. (2016). The Roles of Matrix Metalloproteinases in Anterior Regeneration in *Aeolosoma viride* (923.2). The FASEB Journal 30 (1 Supplement)

Tseng, T. L., Chen J. H. (2014). Cloning, expression and characterization of two fibrinolytic enzymes from fresh water annelid, *Aeolosoma viride*. 10th International Symposium on Earthworm Ecology - ISEE 10.

Visse R., Nagase H. (2003). Matrix metalloproteinases and tissue inhibitors of metalloproteinases. Circulation Research. 92, 827-839.

Wang, X., & Page-McCaw, A. (2014). A matrix metalloproteinase mediates long-distance attenuation of stem cell proliferation. J Cell Biol, 206(7), 923-936.

Weidhase, M., Bleidorn, C., & Helm, C. (2014). Structure and anterior regeneration of musculature and nervous system in *Cirratulus cf. cirratus* (Cirratulidae, Annelida). J Morphol, 275(12), 1418-1430.

Woessner, H. N. a. J. F. (1999). Matrix Metalloproteinases. The Journal of Biological Chemistry, 274, 21491-21494.

Wong, H. L., Jin, G., Cao, R., Zhang, S., Cao, Y., & Zhou, Z. (2016). MT1-MMP sheds LYVE-1 on lymphatic endothelial cells and suppresses VEGF-C production to inhibit lymphangiogenesis. Nat Commun, 7, 10824.

Wu J, Lu M1, Li Y, Shang YK, Wang SJ, Meng Y, Wang Z, Li ZS, Chen H, Chen ZN, Bian H. (2016). Regulation of a TGF-beta1-CD147 self-sustaining network in the differentiation plasticity of hepatocellular carcinoma cells. Oncogene.

Wu X, Deng G, Hao X, Li Y, Zeng J, Ma C, He Y, Liu X, Wang Y. (2014). A caspase-

dependent pathway is involved in Wnt/beta-catenin signaling promoted apoptosis

in Bacillus Calmette-Guerin infected RAW264.7 macrophages. Int J Mol Sci,

15(3), 5045-5062.
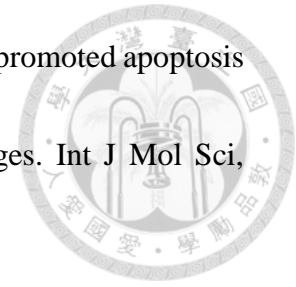
Yong, V. W. (2005). Metalloproteinases: mediators of pathology and regeneration in the

CNS. Nat Rev Neurosci, 6(12), 931-944.

Zhang, Z., Song, T., Jin, Y., Pan, J., Zhang, L., Wang, L., & Li, P. (2009). Epidermal

growth factor receptor regulates MT1-MMP and MMP-2 synthesis in SiHa cells

via both PI3-K/AKT and MAPK/ERK pathways. Int J Gynecol Cancer, 19(6),

998-1003.

Zoran, M. J. (2010). Regeneration in Annelids. doi:10.1002/9780470015902.a0022103

37

Figures

A

```
G TAG ACC TAT ACC AGG AAT TTC AAG CGA AAA CGT TAT AAA ACT TTT AAA CTC ATG CGA CAG AAT ATA CGC TTC ATT TAA AA
                                                                                                    ORF
T GTT TGA CTC GAT TTA CGG TTA CTG CAG CAC GAA CGC ATC GGG TTT ACT TTT GAT CGC AAC ACT ATG ACT GGA GAG CGA GG
ORF
A TAT TTT TCA GTG AAC ATC TTC ATG GGC CTA GGC CTG ATC TGT TTC GTT CTG ATG TGT CAA TTG TCT TAC GCA GCG CCC AT
ORF
C ACA GAT GAA GAA AAC GCT AAG GCT GAA GAA TAT TTA AAA CAA TTC AAT TAC ATG AGG CAG CCG AAA GCT GCA GAA AAT TC
ORF
T TTA ATT GCT GGC TTG GTT CAA CTG CCT CCA AAA ACA AAC ACA AAC GAT GCT CTT GAA AAG TTT CAG CGG ATG TGG GGC TT
ORF
A AAA GCC ACA GGA AAA CTG GAT GAT GCA ACA TTG GCG TTG ATG AGT AAA CGA CGA TGT GGT GTG CCC GAC ATC ACC AAC TC
ORF
C GAA GAC GAC GAA CGA AAA AAA CGC TAT GTT ACT ATA GGT AAT AAA TGG GAC AGG ACA AGC TTG ACT TAC AAA ATT AAC AA
ORF
T TTT ACT CCC GAT ATA TCG TCA ACA TCT TCT GTA ATA AAG GAC ATA GAA CAG GCT TTT AAA CTG TGG AGT GAC CAG ACA CC
ORF
G CTT ATA TTC AAT CGC ATC ACT AGT GGT AAA GCA GAC ATT GAA ATA TCA TTC GCA AGC AAA GAT CAC GGT GAC GGT AGT GC
ORF
A TTT GAT GGA CCC GGT GTA GTC CTC GCG CAT GCT TTT TTT CCT CAG CAG GGA GCT ATT GGA GGA GAC ACT CAT TTC GAT GA
ORF
G GAT GAA CGA TGG TCA ACA TCT GGC TCT ACA GGA GTC GAT CTC ATG CAA GTC GCA GCG CAT GAG TTT GGT CAC GCA TTA GG
ORF
A CTA AGT CAC TCA GAA AAC ATG GAC GCC CTA ATG GCT CCT TTC TAC AGA GGA TAT GTT GCG AAT TTC CAA CTA AAC GCA GA
ORF
T GAC ATC CGC GGC ATA CAG GCA ATA TAC GGT TCT AAG GCA CGT TAT CCA GTA GCT CCC ACC AGA ACG ACT CCA ACC ACT AC
ORF
G ACA ATT GCA ACG AGA ACA TTA TCA AGA ACA ATG AGA CCA ACA ACA ACT ACG CGC CCT CCT TTA CCG GAA GTT TGT CGC GT
ORF
T GCC AAA TTT GAT GCC ATA ACA CAA ATG GAA GAC GGA AAT CTT TAT GTA TTT GCC GGT GAC AAA TAT TAC AAA ATA ACC GC
ORF
A AAT GGA CCA GCT CCA GGT TAT CCC CGT TAC ATT AGC AGA GAT TTT CCA GGT GCG CCA AAC AAT TTG AAC GCT GCT GTT TC
ORF
C GTG TCA GCA CTG AAA TAT GGA GAA ACA TCA TAT ACC TAC TTA TTT AAA GAT GAA AAA TTT TGG AAA ATC GCT AAT GCT GT
ORF
T GTA AAA GGA ACG GGA CTA ATA GCC AAT GAA TTT CCT GGT ATA CCT CCT TCA GTG AAT TCT GCA TTT ACT AAT GCC TTG AA
ORF
A GGC GAT ATC TAT TTC ACG CAA GGT AGT ATG TAC TAC AGA TTT GTT CGT TAC GCT CGT GAA CAA GGA GTT GCT GAA GGG TA
ORF
T CCG CGT TCG CTA CTT TTG TTA AAG GGA CTT CCA AGT ACA ATT GAC AAC GCC TTT GAA TGG GAT AAC AAG AAT TAC TTT AC
ORF
C AAA GTA TCC AGT GTC TAT CGC TAT AAC TAT CAA CAA GAT AAG GTA GAT GAT GGT CCG AAG AAT TTT GCT GAC GAA TGG TT
ORF
A AAA TGT AAT AAG GGG TTG AGA TCT TTC GAA TCC CCG GAG ACA GAA AGC GGC GCA TCA TCA AAC ATT TGT TAT TTA ACG AC
ORF
A CAA CTG TAC TGT ATT ATC TTC TTA GCT CTT ACT GTC TTA CTA ACG ATT GGC GAG TTA TGA TAA GAC ATT CTA TGA AAT GA
A AAT ATT ATT TGT TTT ACA TTA CTT TTT GAT GCG TTT GTA CCA GGC AGT TAA GTA AAA TGT AAG AGA TGT TTT TAA ATC AT
A CAT TCG CAT GTT TTA CAC TTT AAG AAT ACA TTT AGT TTA GCT ATA ACG ACA ATT AAT GGC TAG AAA ATA AGT TGA TTG CA
T AAT GCA AAT TAT CGA TAT ATA ACT AGT ATG CAT TGT GCA TTG TGC ATA TTG TGC ATT GTG TAT TGT GCA TTG TGT ATT GT
G CAT AAT GTT TTA TGC ATT GTG CAT AAT GTC TTG TGC ATT GTA CGT TAT GCT TTA TAC TTA AAT ACG AAT TTT TAT CAT TG
A AGA TTG TCA AAC TCA TGA AAA GAT GTT ACA TTA CAG AGA CTA ATA TAG AAT TTA ACT GCG CAG TTA AAT ACT TAA GAT AC
T AAT AAC ATA AAA CTC AAT GTA GCA CAC CTA AAT ACT GAA G
```

38

B

```
                    20                        40                        60
                    |                         |                         |
MTGERGYFSVNIFMGLGLICFVLMCQLSYAAPITDEENAKAEEYLKQFNYMRQPKAAENS

                    80                       100                       120
                    |                         |                         |
LIAGLVQLPPKTNTNDALEKFQRMWGLKATGKLDDATLALMSKRRCGVPDITNSEDDERK

                   140                       160                       180
                    |                         |                         |
KRYVTIGNKWDRTSLTYKINNFTPDISSTSSVIKDIEQAFKLWSDQTPLIFNRITSGKAD

                   200                       220                       240
                    |                         |                         |
 IEISFASKDHGDGSAFDGPGVVLAHAFFPQQGAIGGDTHFDEDERWSTSGSTGVDLMQVA

                   260                       280                       300
                    |                         |                         |
AHEFGHALGLSHSENMDALMAPFYRGYVANFQLNADDIRGIQAIYGSKARYPVAPTRTTP

                   320                       340                       360
                    |                         |                         |
TTTTIATRTLSRTMRPTTTTRPPLPEVCRVAKFDAITQMEDGNLYVFAGDKYYKITANGP

                   380                       400                       420
                    |                         |                         |
APGYPRYISRDFPGAPNNLNAAVSVSALKYGETSYTYLFKDEKFWKIANAVVKGTGLIAN

                   440                       460                       480
                    |                         |                         |
EFPGIPPSVNSAFTNALKGDIYFTQGSMYYRFVRYAREQGVAEGYPRSLLLLKGLPSTID

                   500                       520                       540
                    |                         |                         |
NAFEWDKNYFTKVSSVYRYNYQQDKVDDGPKNFADEWLKCNKGLRSFESPETESGASSN

                   560
                    |
 ICYLTTQLYCIIFLALTVLLTIGEL*
```

C

D
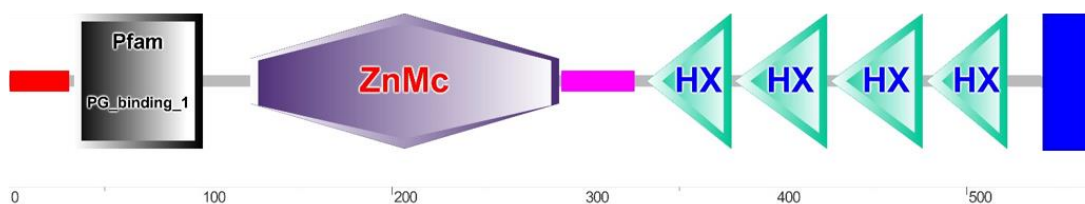
```
                          20                           40                               60                              80
GCA GCT GTC CCG ACA CAT TTT GGC GCG TGT TCG TGC GTT AAT TCA TTG AGG AAC ATT TAA GGA CAG CTG CCT AGG TCA ACG
                       100                           120                              140                             160
GTA GGT ACA ACA GCA ATA AAA CTT AAA TGA AGA GTT CTG TTA ACA CGT CGT TAA CGT AAA AAG GCC CTT TGA CCG AAA GCT
                       180                           200                              220                             240
CAT CGA CAC ATT GAA ACG ACT TCA TTG AAA CAA TAG CTA TTG TGA GAG CCG GCC TGA CTG ACT GCC ATA AGC GCC ACC TCG
                       |ORF
                       260                           280                              300                             320
CAT CAT GTT TTA ATG TTG TTA CGA GTA AAA CAA CTG CAA ATT TCC GCG TCA TCG TTA TTA AGA AAA GAA ATG GTA GCC ACT
|ORF
              340                           360                              380                             400
TCG TCG CAT CAA GTC GAT GAT CAT GAT AGC TGT CGC CAT CTA GAG AGT GAC GAG GCA GCT AAT ATT CAT CGT TTT TAC TCG
|ORF
              420                           440                              460                             480
TTA CAT GAC GCC TCC ATT TCA TCA AGC CAG CAA CGT CGC TGT GGT GCG CTG GCT GAT ACT GCT GCT ATT GCT GAT AGT TTT
|ORF
              500                           520                              540                             560
TGC TGC CGG AAA TGG TGG CCC AGA GTG AGT CGT CAT CAA CTT CTC AGC CTA CTT CTG TGC CAA CTG CTT TAT TTG GCT TGC
|ORF
              580                           600                              620                             640
CCA TCA TAT GGC TTG CCA ACT CAC TTC AGT TCG TCT CAT CAC AGG CTA AGA ACA GCC AGC AGA ACA ACT AAT ACA AAC AAT
|ORF
              660                           680                              700                             720
AAC AAC AAC ACA GGC ATT GAT AGC TCG ATG TAT CTG ATG CGG TTT GGC TAT CTG CCT CAG TCA GAC ATG GAG ACG GGT GCA
|ORF
              740                           760                              780                             800
CTA CGT TCC AAG GAA GAG TAC GAG TCT GCT GTG AAA CGC TTC CAG AGA TTT GCA AAC TTG CCG CAG ACG GGA CAG CTA GAT
|ORF
              820                           840                              860                             880
ACG GCT ACG CTG GCT CAA ATG CGC AAG CCC CGC TGC GGT CTG CCA GAC GTG ATG CCA GAG ACG AGA CAG ATC GTG ACA TCA
|ORF
              900                           920                              940                             960
CAA CAG ACG ACG AGG GGC AGA AGG CAG CGC CGA TAC GTG CTC GGC CCG AGC AAG TGG CCG AAG ACA GAT CTC ACT TTT CGG
|ORF
              980                           1,000                            1,020                           1,040
ATA TTA AAT TAT TCC CCG GAT TTG ACA AGC AGT GAA ATA CGC ACA GCC ATC TAT CGA GCA TTG AGA GTA TGG AGT GAC GTT
|ORF
              1,060                         1,080                            1,100                           1,120
AGT CAG CTA AAT TAT CGC GAA GTA TTT CAG CAG GAA TCG GAC ATA GAA ATA CTA TTC GCT TCT GGT TAT CAC ACA GAT GGC
|ORF
              1,140                         1,160                            1,180                           1,200
CAT CCT TTT GAT GGA CCT GGA ACT GTA CTT GCT CAT GCC TAT CCA CCA GGA GAT GAA AAA GGT GGA GAT GTT CAT TTC GAC
|ORF
              1,220                         1,240                            1,260                           1,280
GAG GAC GAA AAT TGG ACT TTC AGT TCT TAC GAA GGT ATC GAG TTA TTC ACA ACT GCA GCA CAT GAA ATT GGG CAT GCT CTC
|ORF
              1,300                         1,320                            1,340                           1,360
GGA CTT TAT CAT TCC GAC GTT CCA GGA TCC TTA ATG GCC CCT TGG TAT CAA GGA TAT AAT CCG GAT TTC AAG TTA TCT GAT
|ORF
              1,380                         1,400                            1,420                           1,440
GAT GAC ATT GCC GCA ATA CGT CAT CTT TAC GGC TCT CGC TCT CCC TCA ACA ACG ACA ACA AAA TCC CCA GCA ACG ACA AGG
|ORF
              1,460                         1,500                            1,520
TCG ACA ACG ACA AGA AAA TCA CCA GAT GGC GGT ACT ACC ACC ACC ACT ACA GTT GCA ACT ACA ACA ATC AGA AAA CCT AAG
|ORF
              1,540                         1,560                            1,580                           1,600                1,620
ACA AGT GCT GCA ACG ACA ACT CCA TCG GTG CAG GAT AAG CGC AGC CGC ATC ACT GCA ACA CAG ACC TCG ACG CCG TGT CCG
|ORF
              1,640                         1,660                            1,680                           1,700
TCA TCC GAG GCG AAT TAT TCG CAT TTA AAG ATA AGT GGT TTT GGC GCC GTA ATA AAA ACG GCG ACA TGA ATG AAG TTC CTG
              1,720                         1,740                            1,760                           1,780
CAG AAT TGG GCC AGT TCT GGT ATG GCT TTC CTA ACG ACA TTA CCT CAA TAG ACG CCG TGT TTG AGA GAC CAA GTG ATG GTC
              1,800                         1,820                            1,840                           1,860
AGA TTT GCT TCT TCA ATG GCA ATC GTT ATT GGT TCT TTC AAG GTA ATC AGT TGG CTG CAG GCT TTC CGA AAA CTG GTC GCT
              1,880                         1,900                            1,920                           1,940
TGT TGA CAA CTC TTG GTC TTC CCG ATG ACA TTG AGA AAG TAG ATG CAG CCT TCG TCT GGG GAC ATA ACA AGC GTG TCT ACT
              1,960                         1,980                            2,000                           2,020
TGA TCA GTG GTA ACA TGT ACT GGA AGC TGA ATC CAG ATG CCA CCG GCA TCG AAG CTG GTT ACC CTC GAG ATA TGG AAA TGT
              2,040                         2,060                            2,080                           2,100
GGG CTA ATG TAC CTC TGC CTG TAG ATG CTG CCT TCT TAT ACT GGA ATG GTA ATA CTT ACT TCT TGC GAG ATC AGT TCA CCT
              2,120                         2,140                            2,160                           2,180
ATG AAT TTA GCG ATG TCA AGA TGA ATG TGA GAG AGG CTG GCA TGA GAC AAA TGG CCA GCC ACT TAT TTA GCT GTC CCG ATC
              2,200                         2,220                            2,240                           2,260
GAC CAA TAA GCT CAC CTC ACA ATG ATG CAC CAG CAA CAG CTA CCT TCC AGC GAA TAA CCT TAT CTA ACT ATT GCT TAC TAC
              2,280                         2,300                            2,320                           2,340
CTC TGC TAA CAT TGT CAT TTA ATT TTC TAC TAC CAC GAA TTT CGA TCG ACT TTT AAA CTC TTA TAT ATT TTT ACG TTT TTT
              2,360                         2,380                            2,400                           2,420
TCT GTA TAT AAA TAG CCG CGA AAA AAA TCG TTA ATT GTG CTG TCT GAA GTA ATT ACA TAA CCC AGT CTT GGA AAC GAC ATC
              2,440                         2,460                            2,480                           2,500
TTT AAC ATT CCA GTA ATC TGA AAA TGT AAA TAA AAT AAG TTA ATT AGA AGC ATC TAT ACA TAA ATT TGC ATG TAC ATT TGT
              2,520                         2,540                            2,560
GCG TGT TTG TGT GCA TGC ATG TAT ACA CAC TTA CAT GCA TAT GCA TAC ATA CAT ACA TAA GCC
```
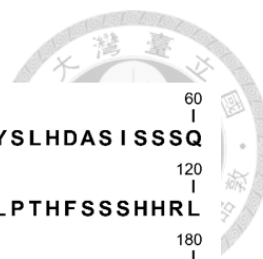
40

E

```
                 20                        40                        60
                 |                         |                         |
MLLRVKQLQISASSLLRKEMVATSSHQVDDHDSCRHLESDEAANIHRFYSLHDASISSSQ
                 80                        100                       120
                 |                         |                         |
QRRCGALADTAAIADSFCCRKWWPRVSRHQLLSLLLCQLLYLACPSYGLPTHFSSSHHRL
                 140                       160                       180
                 |                         |                         |
RTASRTTNTNNNNNTGIDSSMYLMRFGYLPQSDMETGALRSKEEYESAVKRFQRFANLPQ
                 200                       220                       240
                 |                         |                         |
TGQLDTATLAQMRKPRCGLPDVMPETRQIVTSQQTTRGRRQRRYVLGPSKWPKTDLTFRI
                 260                       280                       300
                 |                         |                         |
LNYSPDLTSSEIRTAIYRALRVWSDVSQLNYREVFQQESDIEILFASGYHTDGHPFDGPG
                 320                       340                       360
                 |                         |                         |
TVLAHAYPPGDEKGGDVHFDEDENWTFSSYEGIELFTTAAHEIGHALGLYHSDVPGSLMA
                 380                       400                       420
                 |                         |                         |
PWYQGYNPDFKLSDDDIAAIRHLYGSRSPSTTTTKSPATTRSTTTRKSPDGGTTTTTVA
                 440                       460
                 |                         |
TTTIRKPKTSAATTTPSVQDKRSRITATQTSTPCPSSEANYSHLKISGFGAVIKTAT*
```

F

G
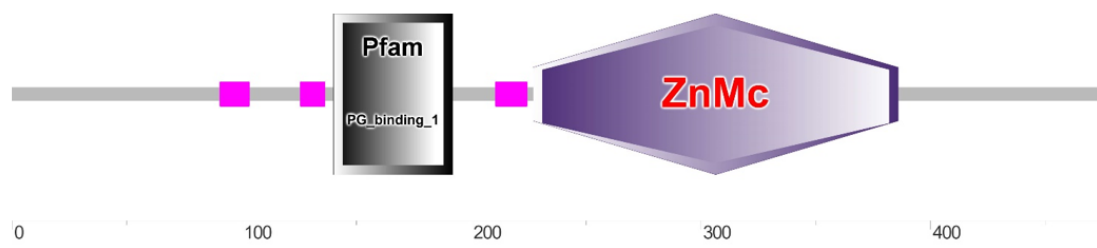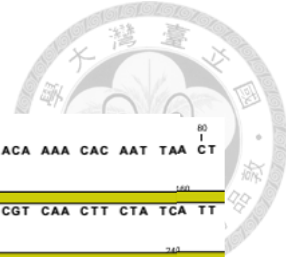
```
            20                      40                                60              80
G CCT TGG CTC ATC TAC GCT CAT TAC AGC AAC AAG GAC GAA TAA AGT GAA GGA GTT GTA CAA AGA ACA AAA CAC AAT TAA CT
                                                          ORF
                        100                     120             140                         160
A GCT TTC GAT AAA CCT TTA TTA ACT GGA ACA ATA TGC ATC ATG AAG ATG GCA CTG CAT TCG TCT CGT CAA CTT CTA TCA TT
ORF
                180                     200                     220                     240
T CTT AAC CAT CGC TTA CCC CAG ACG TTT CGT TCC GTG CGT CTG TGT CAG CTG CTG CTG CTG CTG CAG CTG TTA TTG CTG GC
ORF
                260                     280                     300                     320
G CCA AAG AAC TCG CTG GCT GAT GAC GCG CAT GAG ATG CGT AAC GTT CAC CTA GCC ACA CAG GTG ACG AGC GAG GAT ACC AA
ORF
                340                     360                     380                     400
T GGA GGC TTT TTC ATA GAT ACA TAT GAA AAG GCT TTG ATG TAT CTA AAG AAA TAC GAC TAT CTT AAC TGC ACG CTA GTG CT
ORF
                420                     440                     460                     480
A AGC AAA CGC AAA CGA CGC GAC GTG GAT CAA ATG ATG CCG TTT TTC GAA GTC AAC GAA CTT TTA GCC ACT GTC ACG CAC GA
ORF
                500                     520                     540                     560
G CCG TCG TCA CTG CCC CCG TGC AAC GAT TTA GAC ATT TTC GCA GCT TTC GTC GAG TTC CAA CAG AAA TTC GAC CTG CCA AT
ORF
                580                     600                     620                     640
A ACG GGC TCA TTT AAT GAC GAC ACA GCT CGG CTG ATG AGT GCC GGA AGG TGC GGC AAC ACC GAC CAC GAC CAC CAG TCC CC
ORF
                680                     680                     700                     720
T GAT GAG GAG ACT AAT ACT GTC AAA TCT GCT CTT CTA ACC AAC GCT CGG CGC AAA GAT GAG CAC ATT GAT GGC GAC GCG CC
ORF
                740                     760                     780                     800
G CAC CAC TCC GTG CGT CGG CGT GCA GCG AAT TTA TTG TTA CGG AAG AAA CAT GAG GTA GGC AAT AAT GGA GCA GTT CAC CA
ORF
                820                     840                     860                     880
G TCA CAT TTC AAC ATC GAT GTG GGG TTA AGA CAG TTA ATG TGG CGC AAA GCC ACA GAA CGC ATT CAA CGG CGA TAT TCG CG
ORF
                900                     920                     940                     960
T GGC CAA CGA AGA AAT GGC CCA CTC TTT GAA GCT GAA GAA GCA GAG GTT TCC GAT GTC TTT GGT ACC CAA GAA GCG GCG GA
ORF
                980                     1,000                   1,020                   1,040
A AAG AAG GAA GCA CAA TCT ACT GGC ATG CAC CAG TGG ATG CGT ATC CGA AAA CGT CGC GAA ACA TTG GCT CCT TCG GAG AA
ORF
                1,060                   1,080                   1,100                   1,120
T TAT ACA GTC AAC GAA GAA CTG CTG AGT GGT ATC TAC ACC AAG TTT AAT AAA GAA TAC GGC CAG CCG ATC ACC TGG CGC GT
ORF
                1,140                   1,160                   1,180                   1,200
G TTA GAA ATG GCG CAC AGC GCC AAA ATC CGA CAA GCG GAG CTG CGA GAA ATC ATG CAA ACA GCT TTT CGC ATC TGG TCT GA
ORF
                1,220                   1,240                   1,260                   1,280
A GTG ACA CCG GTT GTG TTT GAG GAG AAA AAC ACT GGG CCC ATC GAC ATG GTT GAC ATT GAA ATC GGC TTT GGC AAA CTG CG
ORF
                1,300                   1,320                   1,340                   1,360
T CAT CTT GAC TGT CGC CAC CCG TTT GAC GGG CGA GGC GGT GAG CTG GCT CAT TCC AGT CAG ACG ACA GCT CAC AAA GTT AT
ORF
                1,380                   1,400                   1,420                   1,440
C CAC TTC GAC GAC GAC GAA TGT TTC AAA GCT GCC ACT GCC GTC GGC CAG CCG TGT CTC AAC CTA CTT CCG GTC GCT ATC CA
ORF
                1,460                   1,480                   1,500                   1,520
T GAA ATA GGT CAT GTA CTC GGC CTG CCT CAT TCG GAG AGT CGG CAA TCC ATC ATG TTT CCG GTT TAC GAT CAC AGT AAG AA
ORF
                1,540                   1,560                   1,580                   1,600                   1,620
G AAT TCA GAG TAC GAA TTA TCC ACC GAT GAC CGT CGC AGC ATC CAA GGC ATC TAC GGC GTG TGC AAG CGC GGT GAC TTC TC
ORF
                1,640                   1,660                   1,680                   1,700
G GTC GTC TGG GAT TGG CTA CGT CGT CGC GAC GTG CCC GGC TCG ACG ACA CCG CGC TAC TAC TAC AAT ACT TAC TTC GCG CG
ORF
                1,720                   1,740                   1,760                   1,780
C GAC CGT TGG TTC TGG ATG TAC GAA AAC CGT AAC AAT CGG ACA CGT TAC GGC GAC CCG ATG ACG ATA GCG AAC GGT TGG CC
ORF
                1,800                   1,820                   1,840                   1,860
C GGT TTG CCT GCC ACC ATC GAC GCT TAC TGT CAA GTG CTC AGG CGA GAC GTT CTT GGA CAC TAT GGC ATA GAA ACC TAC TT
ORF
                1,940                   1,980                   2,000                   2,030
C TTC TCG GGT TCA AAG TAC TAC CGC TAT GAT GAT CGT GAA GAC AAA GTA ATG AAT GGT TTT CCT CGC GAC ATT TCA ACA GA
ORF
                2,040                   2,060                   2,080                   2,100
T TTT GGT CCA AAG CCG GGA AGT AAC GAA TCG ATA CCA AAT GAT CTG GAT GCA GCC TTT TTT GAC CAA AGA GAC CAT CTT AT
ORF
                2,120                   2,140                   2,160                   2,180
C TAT TTT TTC AAA GAT GAA TGG GTT TGG GTA TTC AAT CCA AAA GAT GCA AAT GAT CCA ACA AGG GGC TGC TGT GAG AGA AA
ORF
G GTG AGG TTT CGT GAT CTG TTT CCA ATG TTA AAA CGA GAA GAG CTT GTA TTG ACT GGC AAC GTG GAC ACG GTC TAC TAC TC
```

42

ORF

G TTC GCT CAT CAG GGC ATG TAC ATG TTC AAG GGT GCT GAT GTT TAC CTG AAC GCA TTC TAC TTG AAC GGG CCT TCT CGT AA

ORF

C ATG CTT GTG GTA AAC CCT TGG TAT GTG TAC TGG AAA GAC ATT TGC GAT GTA CAG CCA ACC ACT TAA AAT ACA ACA AT

T AAC ATA ACG TAT CTA TTT ATA ATA GCC AAT CAT AAA AAT ATC AAT GAT AAT CGA CTA AAT TTA TTG GTT TTG CAG CAA TA

A GCG TTG AAG TGA AAT GCT TAT AAA TAC TGG CTG ACC TAA TAA GAG TAA AAA CGG TAG TAC TTA TAA TGA TTG ACT AGT GC

C TCA AGA GTA CTT CGT ACT GGC AAG AGT GTA CAA CTA TAT TGG CTA ACC ATA AAA GTA GAA TTG ATT CGA TTG GCT AAC CA

T AAG AGT AGC ACT GAT ATG ATT GGC TAA CCA TTA AAG TAG CGC TGA TAC GAT TGG CTC ACA ATA AAA GTA GAA CTG ATA CG

A TTG GCT AAC CAT AAG AGT AGA AGT GAT ATG TTT TTA TTT TAG TTA TAT GTG TAT AAT ATA GGC TCT AGC CAT ACG TG

T TGT AGT AAC ATG AGC TTA TTG ATT GAT TAG CTG TAA ACG TAG CAG TGG TGT GTT TGT ATT CTG ATT CGT TAA AGC AAC AC

T TGA ATC TCA TCG TTT AGC TTC TGT GTA TTA TTT AAA TTT CTT GAT TTT TGA TAA ATT GTT AAT TAA CAA CTG CAG ATG CC

G AAA TTT TCC AGC GTT AAA TTC AAC TCT TAT GTA TTT GTT TTA TTT CTT AAA GCT GTA AAC TAT TAT TGT TTC TTT ACT GC

A TCA TCG CCT CAT TAC GTG ATC ATA TGT CAT CAT AAA CTT TAA AGG ATA GCC TTT GTT TAT GCA CGA GTT TAA GTG TTT CC

A GAT AGG CCC TAC ACA CAC ACA CAC ACG CAC ACA CAC CCA GAT AGG CCC TAC ACA CAC ACA C

H

```
                    20                    40                    60
                    |                     |                     |
MKMALHSSRQLLSFLNHRLPQTFRSVRLCQLLLLLQLLLLAPKNSLADDAHEMRNVHLAT
                    80                   100                   120
                    |                     |                     |
QVTSEDTNGGFFIDTYEKALMYLKKYDYLNCTLVLSKRKRRDVDQMMPFFEVNELLATVT
                   140                   160                   180
                    |                     |                     |
HEPSSLPPCNDLDIFAAFVEFQQKFDLPITGSFNDDTARLMSAGRCGNTDHDHQSPDEET
                   200                   220                   240
                    |                     |                     |
NTVKSALLTNARRKDEHIDGDAPHHSVRRRAANLLLRKKHEVGNNGAVHQSHFNIDVGLR
                   260                   280                   300
                    |                     |                     |
QLMWRKATERIQRRYSRGQRRNGPLFEAEEAEVSDVFGTQEAAEKKEAQSTGMHQWMRIR
                   320                   340                   360
                    |                     |                     |
KRRETLAPSENYTVNEELLSGIYTKFNKEYGQPITWRVLEMAHSAKIRQAELREIMQTAF
                   380                   400                   420
                    |                     |                     |
RIWSEVTPVVFEEKNTGPIDMVDIEIGFGKLRHLDCRHPFDGRGGELAHSSQTTAHKVIH
                   440                   460                   480
                    |                     |                     |
FDDDECFKAATAVGQPCLNLLPVAIHEIGHVLGLPHSESRQSIMFPVYDHSKKNSEYELS
                   500                   520                   540
                    |                     |                     |
TDDRRSIQGIYGVCKRGDFSVVWDWLRRRDVPGSTTPRYYYNTYFARDRWFWMYENRNNR
                   560                   580                   600
                    |                     |                     |
TRYGDPMTIANGWPGLPATIDAYCQVLRRDVLGHYGIETYFFSGSKYYRYDDREDKVMNG
                   620                   640                   660
                    |                     |                     |
FPRDISTDFGPKPGSNESIPNDLDAAFFDQRDHLIYFFKDEWVWVFNPKDANDPTRGCCE
                   680                   700                   720
                    |                     |                     |
RKVRFRDLFPMLKREELVLTGNVDTVYYSFAHQGMYMFKGADVYLNAFYLNGPSRNMLVK

VNPWYVYWKDICDVQPTT*
```
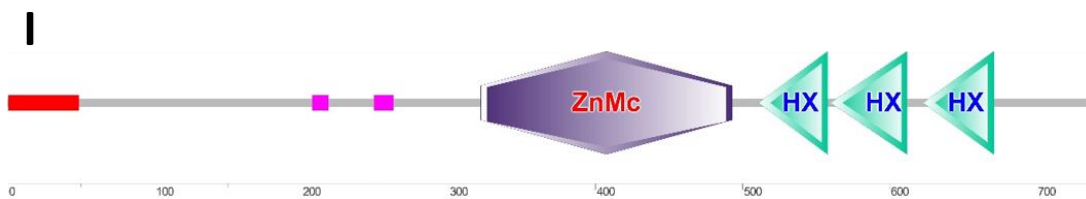
I

Figure 1: Sequences of *Avi-mmps*.

(A) The full length sequence of *Avi-mmp14* is 1698 base pairs, with a 5' UTR of 145 base pairs, a 3' UTR of 466 base pairs and OPF of 1698 base pairs. (B) The predicted polypeptide sequence of *Avi*-MMP14 is 566 amino acids. It is about 63 KD. (C) The protein domain prediction of *Avi*-MMP14. The signal peptide is at first 30 amino acid, marked by red line. The substrate binding domain is at 34-101 amino acid, showed as gray rectangle. The enzyme catalytic domain, zinc-dependent metalloproteinase (ZnMc), is at 126-287 amino acids showed as hexagonal. The hemopexin-like repeat domains are at 333-377, 379-427, 429-477 and 479-521 amino acids showed as green triangle. The transmembrane domain is at 530-560 amino acid showed by blue rectangle. The purple square is the low complexity region. (D) The full length sequence of *Avi-mmp17* is 2574 base pairs, with a 5' UTR of 255 base pairs, a 3' UTR of 885 base pairs and OPF of 1434 base pairs. (E) The predicted polypeptide sequence of *Avi*-MMP17 is 478 amino acids. It is about 53.22 kD. (F) The protein domain prediction of *Avi*-MMP17. The substrate binding domain is at 140-192 amino acid, showed as gray rectangle. The enzyme catalytic domain, ZnMc, is at 227-386 amino acids showed as hexagonal. The purple square is the low complexity region. (G) The full length sequence of *Avi-mmp21* is 3140 base pairs, with a 5' UTR of 121 base pairs, a 3' UTR of 802 base pairs and OPF of 2217 base pairs. (H) The predicted polypeptide sequence of *Avi-MMP21* is 739

44

amino acids. It is about 85.75 KD. (I) The protein domain prediction of *Avi-* MMP21.

The signal peptide is at first 47 amino acid, marked by red line. The enzyme catalytic
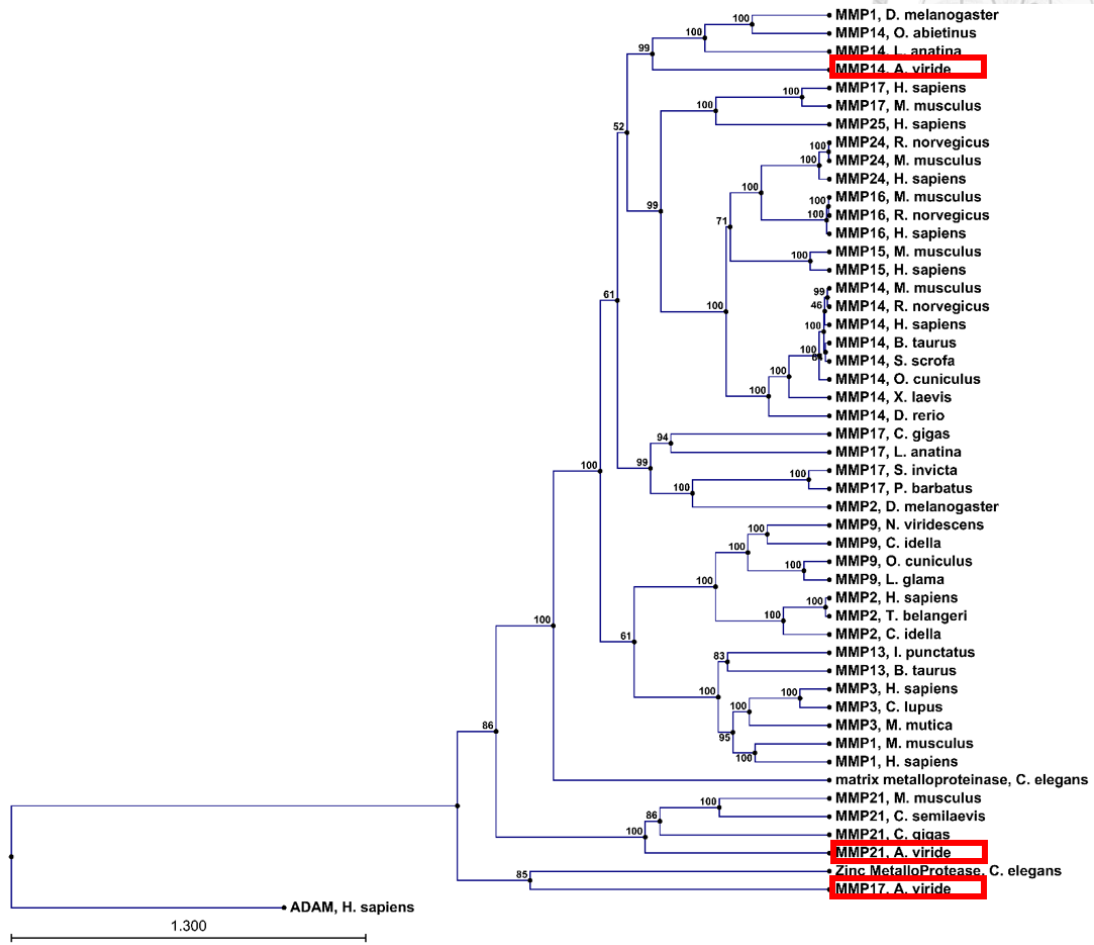
domain, ZnMc, is at 322-493 amino acids showed as hexagonal. The purple square is

the low complexity region. The hemopexin-like repeat domains are at 511-558, 560-

612 and 623-671 amino acids showed as green triangle.
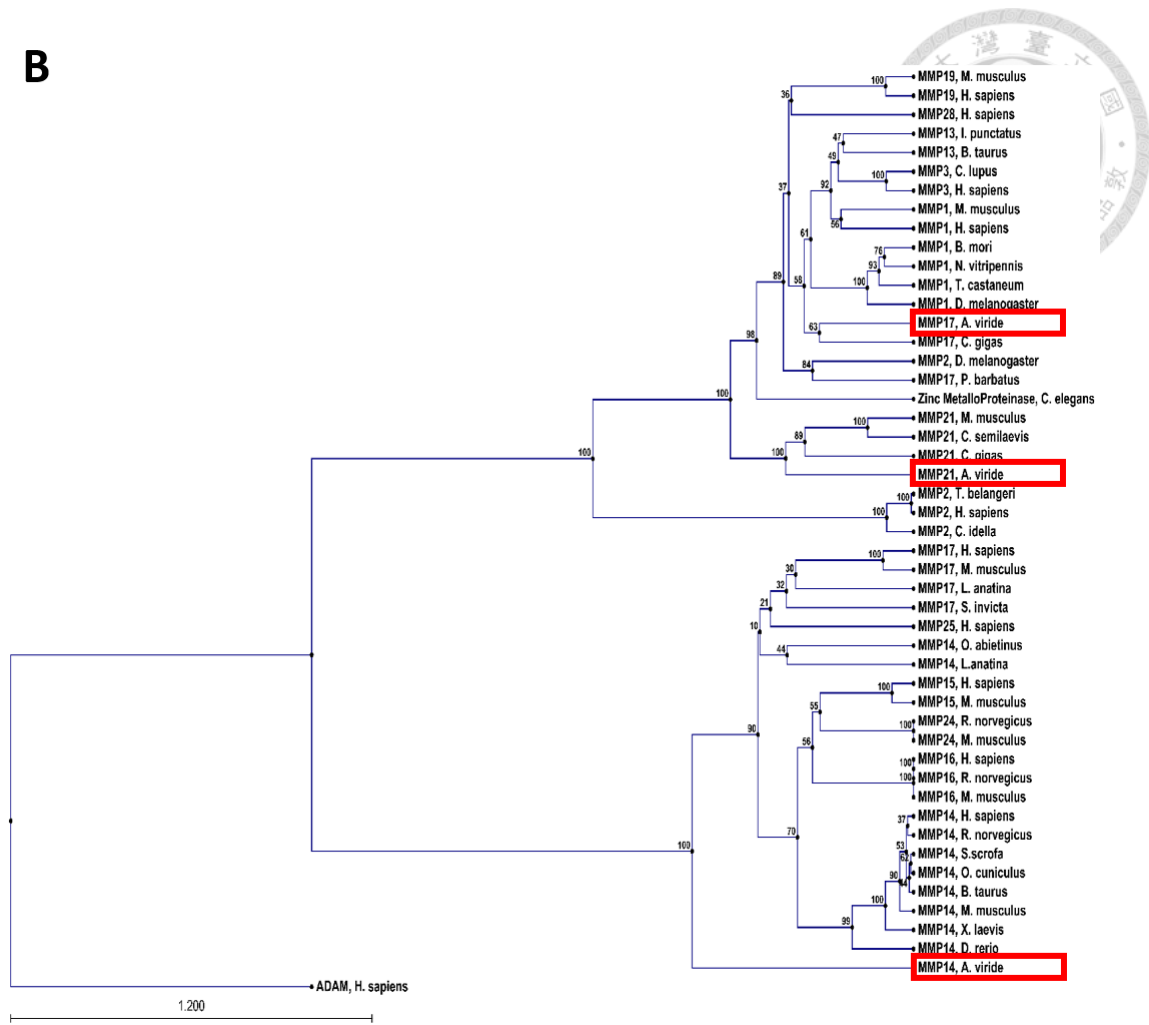
45
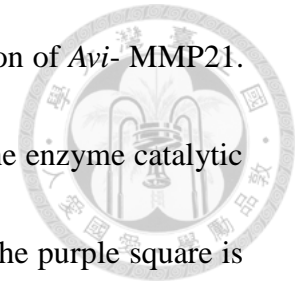
A

B

Figure 2: Phylogenetic tree of *Avi*-MMPs.

(A) The full-length phylogenetic tree of MMPs. ADAM was used as outgroup. *Avi-MMP21* is grouped with MMP21. Both of MMP14 and MMP17 have two groups, invertebrate and vertebrate. *Avi*-MMP14 is grouped with MMP14 of invertebrate. However, *Avi*-MMP17 is grouped with Zinc Metalloproteinase of *C. elegans*. (B) The catalytic domain phylogenetic tree of MMPs. Also, ADAM was used as outgroup. Roughly, MMPs were divided into two group, membrane type and secreted form. *Avi*-MMP17 is grouped with other MMP17 of invertebrate. *Avi*-MMP21 is grouped with MMP21. And *Avi*-MMP14 is grouped with other membrane type MMPs.

48

A

```
G CCA TGG ACA ACA ACA ACA ACA GCA AAA TCA ACT AAA TTG CCA TGG ACA ACA GTG AAT AAA TGG CCA TCA GCT GCA AAT GT
                    20                              40                                  60                              80
T AAT CTA TTT TCC ACA AGA AAT GAA TTA GTA ACA AAA ACT ACG ACA GCG TCA CCC AAA TAT ACA ACA GTT CAC ACA AAA CA
                   100                             120                                 140                             160
T AGA ACA ACT CCT AGT AAA TCA ACC TCG ACT TCA TTT CCT TAT AAT CAA CCC AGA ACT GCT CCG TCC TCA CCG TCG TCG TC
                   180                             200                                 220                             240
G ATA AGA TTC AAT CCT CAG AGC AGA ACC ACG CGC TAT GTA TTC TTC ACG ACG ACC GCC AGA ACC ACT TCC ACA TCT ACT CA
                   260                             280                                 300                             320
A CCA ACG ACA ACC ACA GCG GCC AAA CCT AGT GAT TGT TCA GCA AAA TTT GAT GCA GTT ATT CAA ACT TTA GAC GGA AAA AT
                   340                             360                                 380                             400
T TAC GTA TTT TCT GGC CAA TGG GTA TGG CGT CTC AAT GAC CGA GGC GTA GAA GCT GGT CCG CTA TCT ATA ACT CGC TAC TT
                   420                             440                                 460                             480
C GAA CAA GCT CCG TCT AAT ATC GAC AGT GCT GTA TTT TCA CCG CGG TCC AAT TAT GTA TAT CTA TTT AAA GAT CGT AAA AT
                   500                             520                                 540                             560
C TGG AAG TAT CGA AAC CAG CGT TTA GTT GAA GAA CTC GAG ATT TCC AAC GTG GAT TAT CCA TCC AGT CCC AAA GCT GCT CA
                   580                             600                                 620                             640
A ATT AAC TTA TCG GGA ACG ATT TTT CTG TTT AAG GAT GGT TAT TAT TGG ATT TTT GAC GAA TTC CTG GCC GAT GTA ACT GG
                   660                             680                                 700                             720
C ATT CGT TAT CCA ATG TCG TCA AAA TTC TCC GAC ATT CCT CTC GAC ACT GAG GCA GCA GTT CGC TTA CAG GAT AAT TAC AT
                   740                             760                                 780                             800
G TAC TTC TTC AAA GGC CTA TTA TAT TAC AAG TTT GAT GAG AAT AGT GGC CAT GTG CTA CCT GGT TTA TCC CAA AGA AAA AG
                   820                             840                                 860                             880
C TGG ACC TTG GAT AGG TCC ACA ATG TAA TAA TGG GCG AGC AGA ACC GAA GTA GTA CTG CAT CCC TGA TCA TAC TTT TAA TC
                   900                             920                                 940                             960
A CAA CGA TGC GAA CTT TTA TAA AAT ACG CAA ATA AGC TAC ATA TTT TAT ACA CAT ACA TGA GCA ACA TGA ACG TGC ATA CA
                   980                            1,000                                1,020                           1,040
C ACA TCC ATT CAG ATC TGG ATC CCC
1,050
```

B

```
                                 20                                  40                                  60
                                 |                                   |                                   |
PWT T T T T AKS T KL PWT T VNKWP SAANVNL F ST RNEL VT KT T T ASPKYT T VHT KHRT T PSK

                                 80                                 100                                 120
                                 |                                   |                                   |
ST ST S F PYNQPRT APSSPSSS I R F NPQSRT T RYVF F T T T ART T ST ST QPT T T T AAKPSDC

                                140                                 160                                 180
                                 |                                   |                                   |
SAKF DAV I QT L DGK I YV F SGQWVVWRL NDRGVEAGPL S I T RYF EQAPSN I DSAVF SPRSNY

                                200                                 220                                 240
                                 |                                   |                                   |
VYL F KDRK I WKYRNQRL VEEL E I SNVDYPSSPKAAQ I NL SGT I F L F KDGYYW I F DE F L AD

                                260                                 280                                 300
                                 |                                   |                                   |
VT G I RYPMSSKF SD I PL DT EAAVRL QDNYMYF F KGL L YYKF DENSGHVL PGL SQRKSWT L

DRSTM*
```
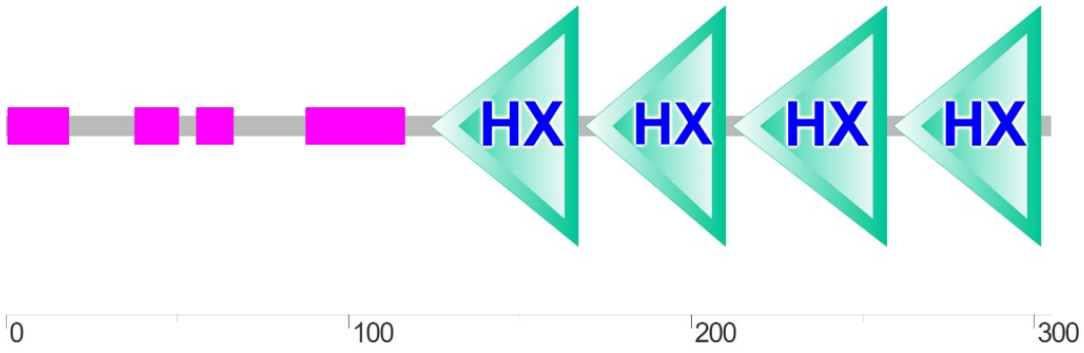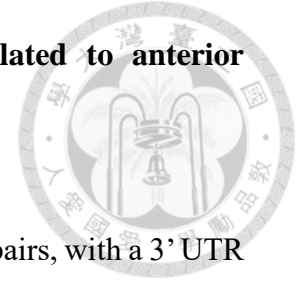
C

49

Figure 3: A MMP-like gene, *Avi*-MMP-like gene found related to anterior regeneration in *A. viride*.

(A) The partial cloned sequence of *Avi-mmp-like gene* is 1078 base pairs, with a 3' UTR of 306 base pairs. (B) The predicted polypeptide sequence of *Avi*-MMP-like gene is 306 amino acids. (C) The protein domain prediction of *Avi*-MMP-like gene. The enzyme catalytic domain has not yet been cloned out. The hemopexin-like repeat domains are at 124-167, 169-210, 212-257 and 259-302 amino acids showed as green triangle. The purple square is the low complexity region.

50
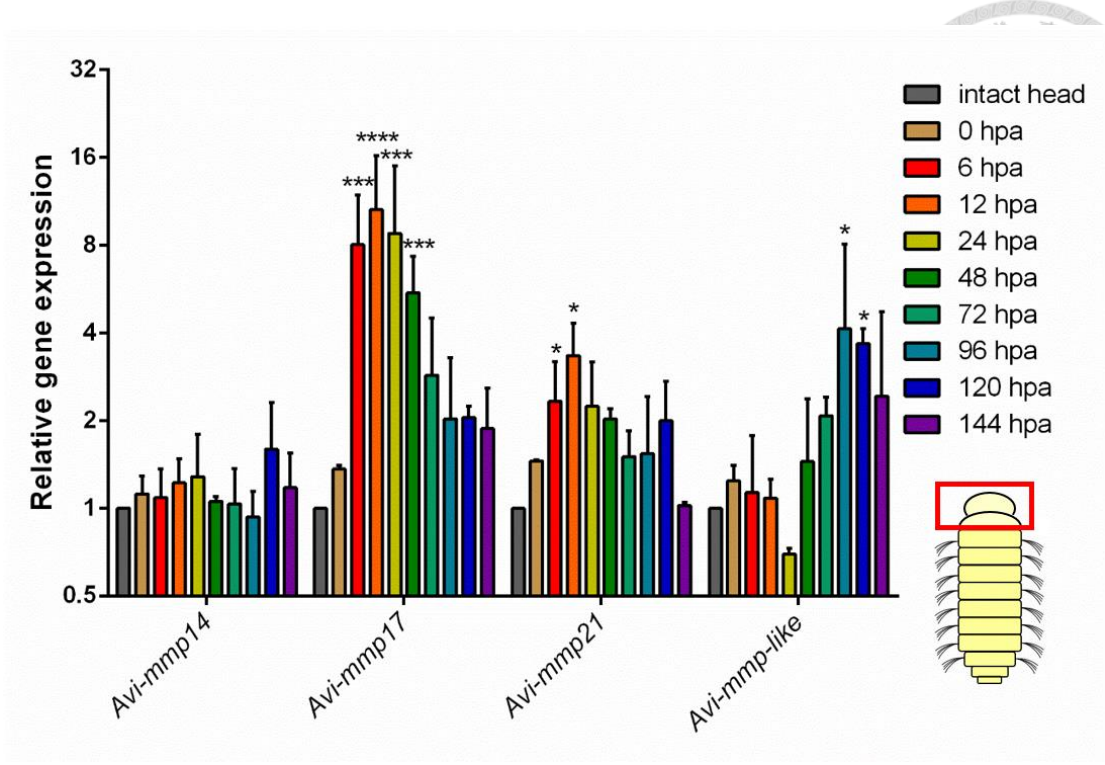
Figure 4: Gene expression of *Avi-mmps* during the anterior regeneration.

The blastema was collected at each stages of anterior regeneration (tissue in the red box). The intact head was used as a control to have relative gene expression during the regeneration. The expression of *Avi-mmp17* increased after 6 hpa and reached highest at 12 hpa about 8 folds relative to intact head. Then the expression decreased to normal after 72 hpa. Also, the expression of *Avi-mmp21* increased after 6 hpa and reached highest at 12 hpa about 4 folds to the intact. Then, the expression slowly decreased after 48 hpa. The expression of *Avi-mmp14* remained stable during the regeneration. And, the expression of one more mmp-like gene, *Avi-mmp-like gene*, decreased before 24 hpa and increased after 48 hpa and reached highest at 96 hpa about 4 folds relative to intact head. Then the expression remained high until the regeneration finished. *: $p < 0.05$. ***: $p < 0.001$. ****: $p < 0.0001$.

A — *Avi-mmp14* (anterior regeneration) sense probe
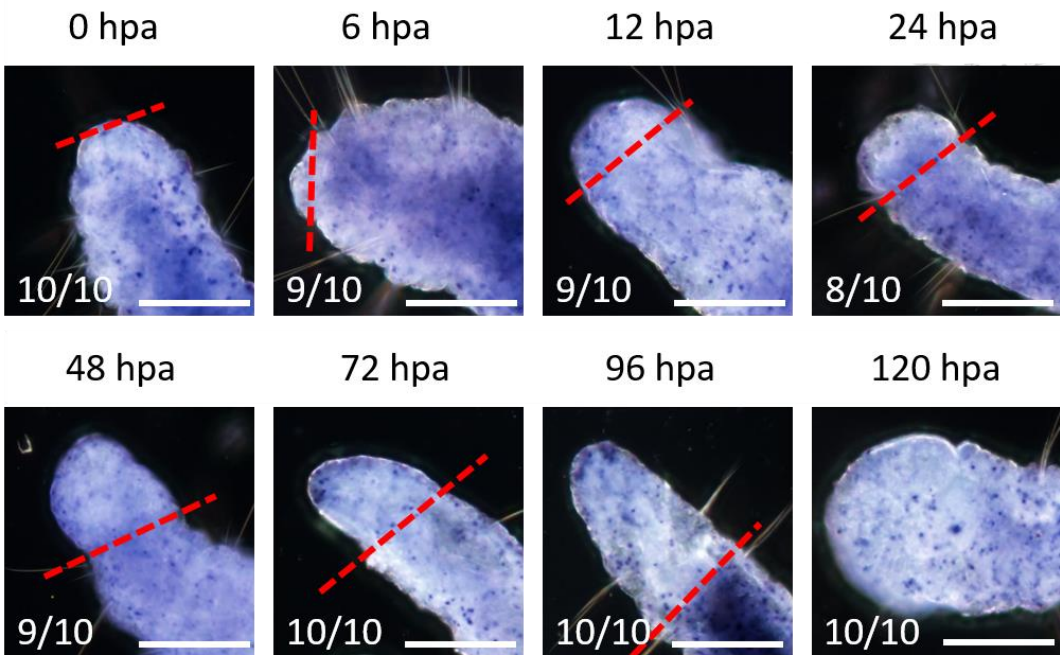
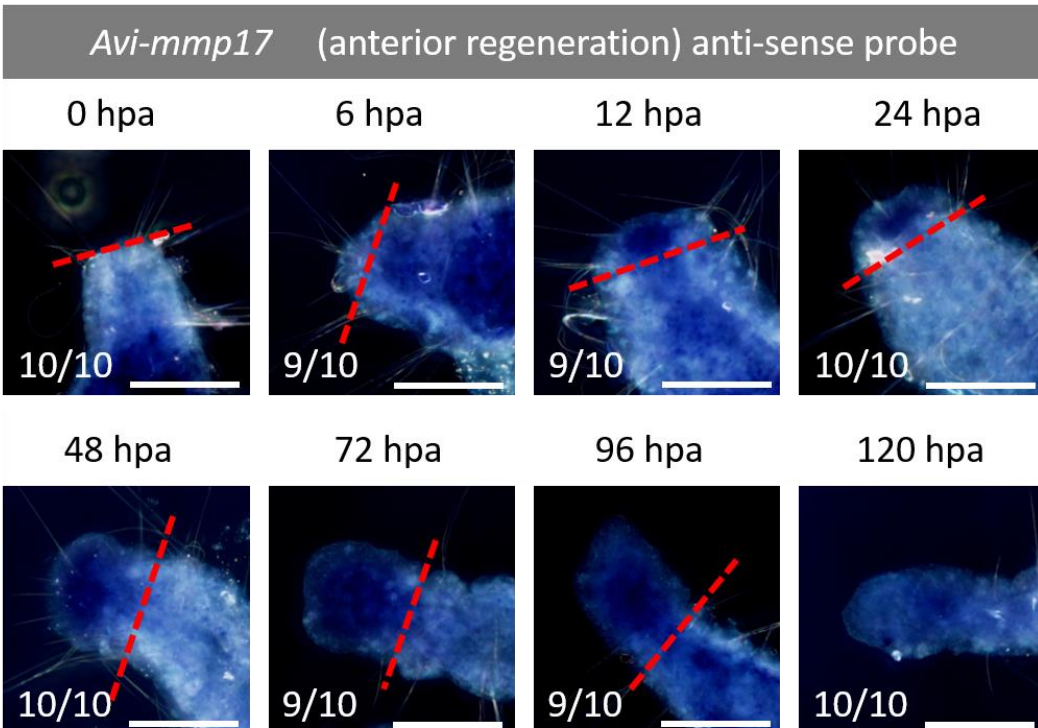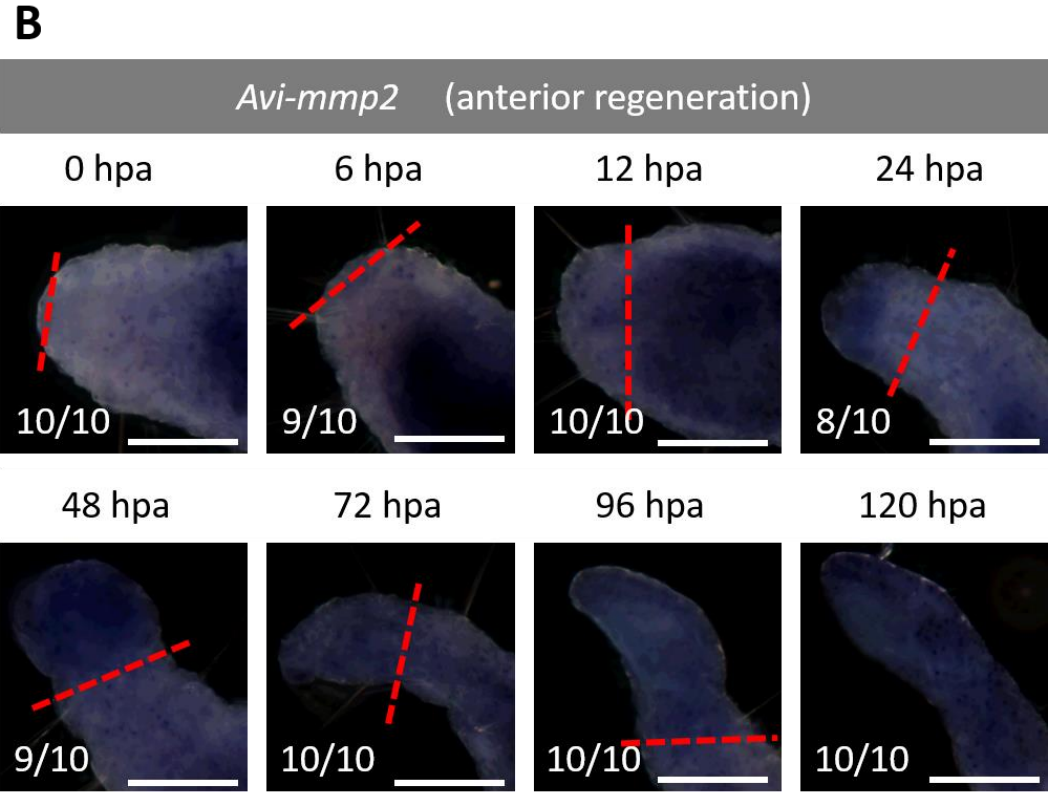**B** — *Avi-mmp14* (anterior regeneration) anti-sense probe
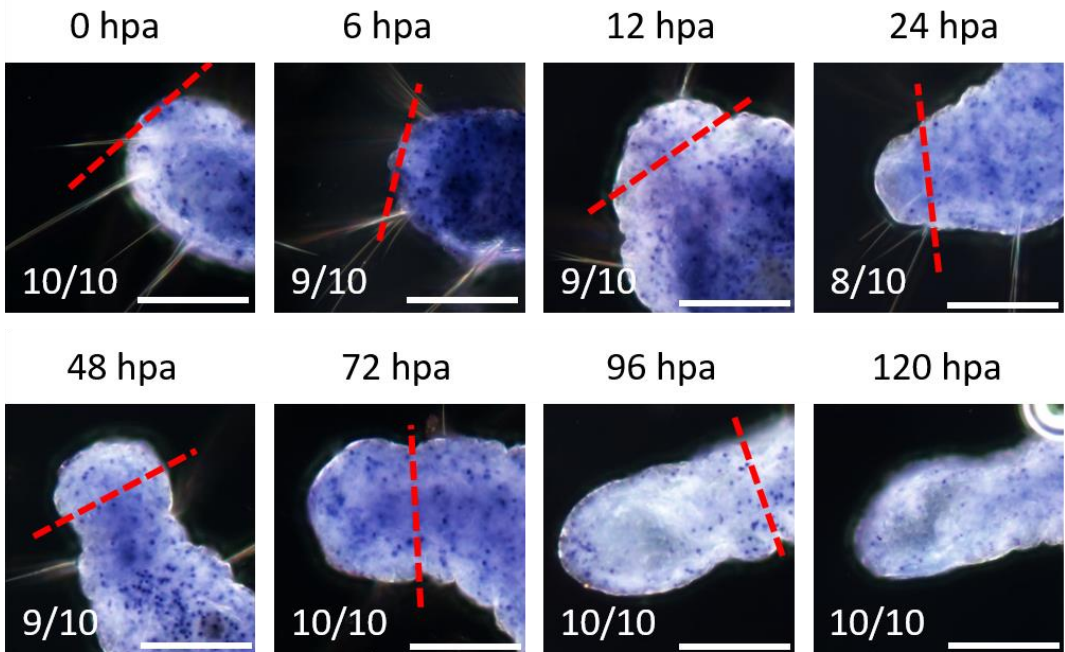
Figure 5: *Avi-mmp14* expressing localization during the anterior regeneration.

(A) *Avi-mmp14* expressing localization in the regenerating worms. Sense probe was used as negative control. (B) During the anterior regeneration, gene expression of *Avi-mmp14* had no significant changes in the blastema, the new growth tissue in front of red dash line. The red dah line is the cutting line. The number at bottom left is the ratio of showed photos in the sample. Scale bar: 100 μm.

A

Avi-mmp17 (anterior regeneration) sense probe

B

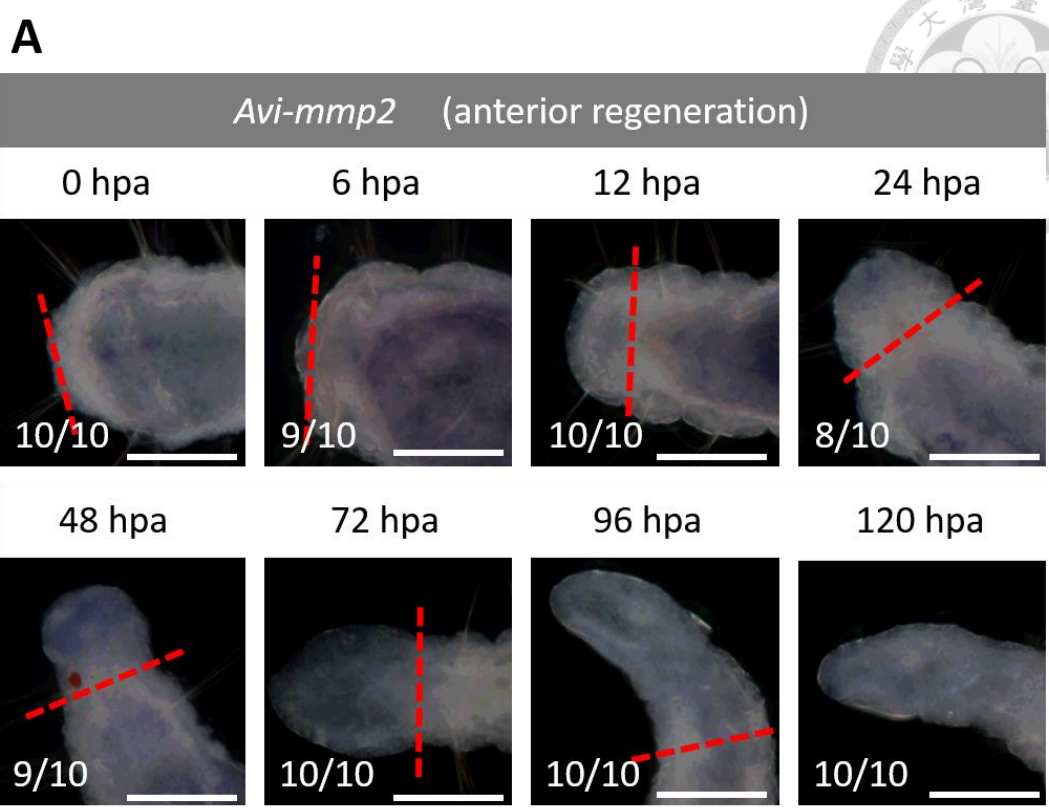*Avi-mmp17* (anterior regeneration) anti-sense probe
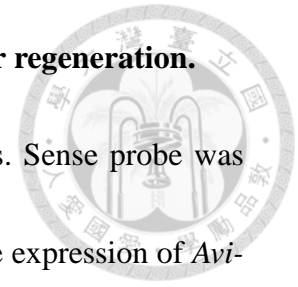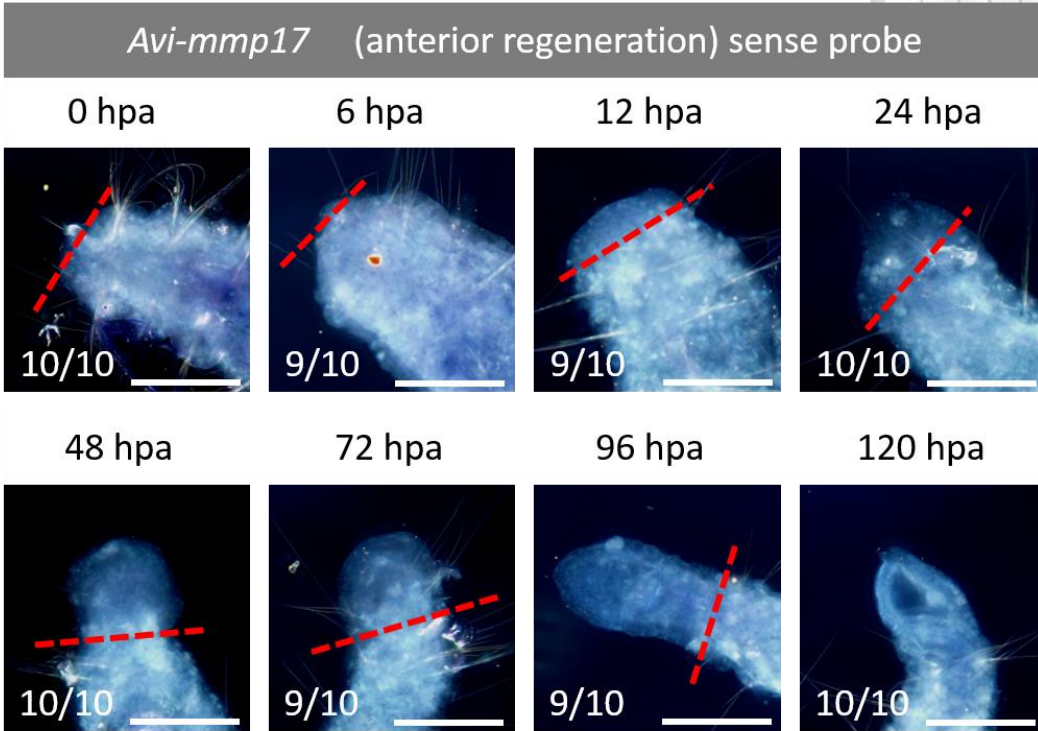
Figure 6: *Avi-mmp17* **expressing localization during the anterior regeneration.**

(A) *Avi-mmp17* expressing localization in the regenerating worms. Sense probe was used as negative control. (B) During the anterior regeneration, gene expression of *Avi-mmp17* can be observed in the blastema after 6 hpa. The gene expression increased to maximum at 24 hpa and 48 hpa. Then, the gene expression decreased after 72 hpa. In 120 hpa, the regeneration completed and the gene expression is similar to the intact worms. The red dah line is the cutting line. The number at bottom left is the ratio of showed photos in the sample. Scale bar: 100 μm.
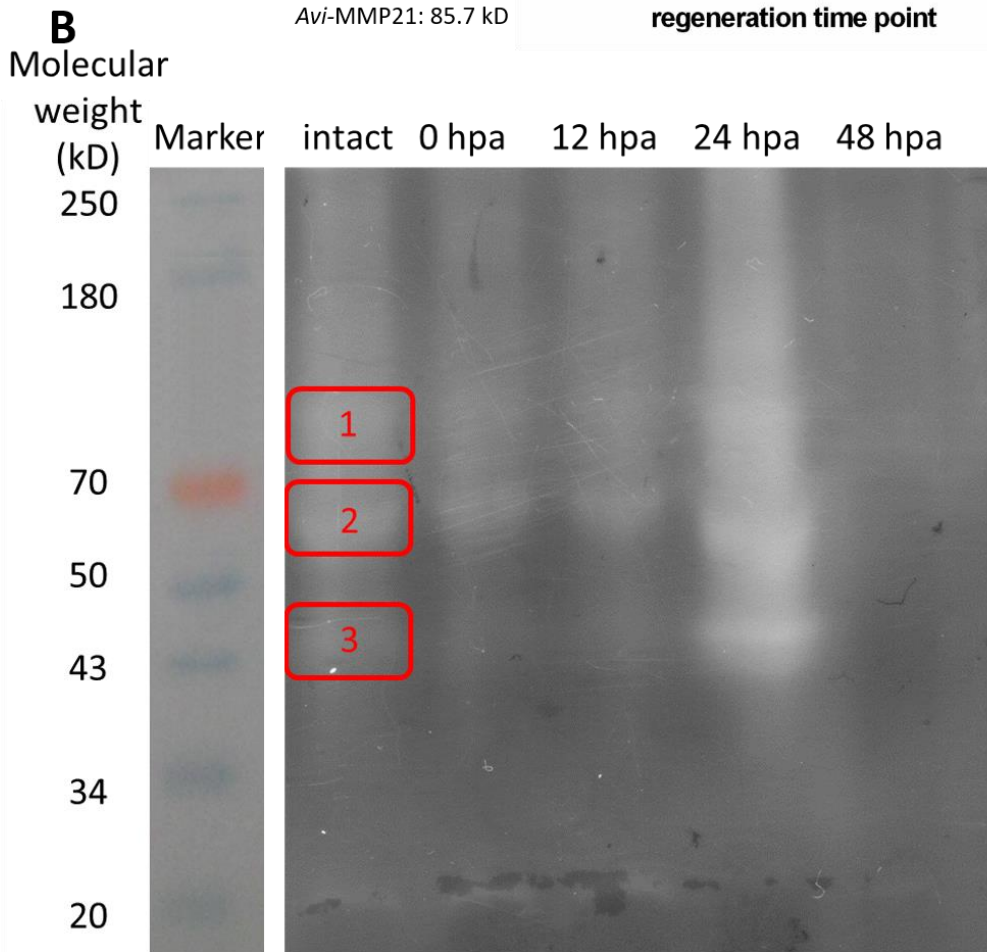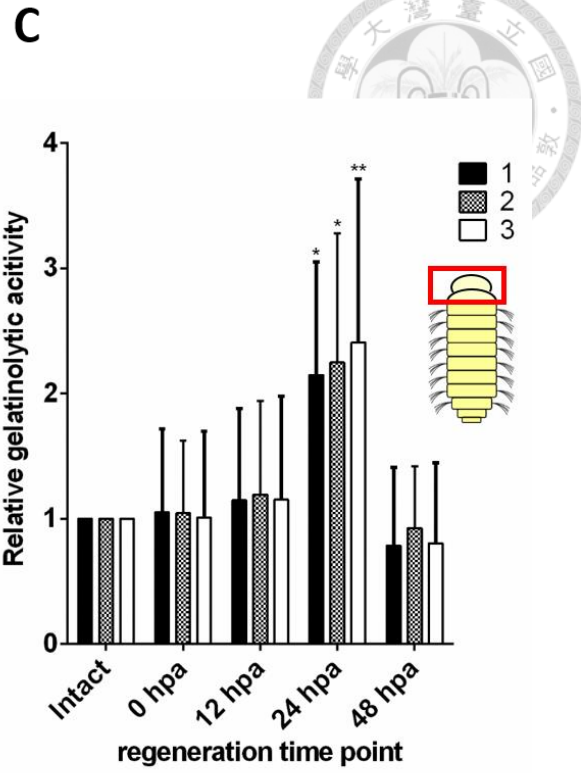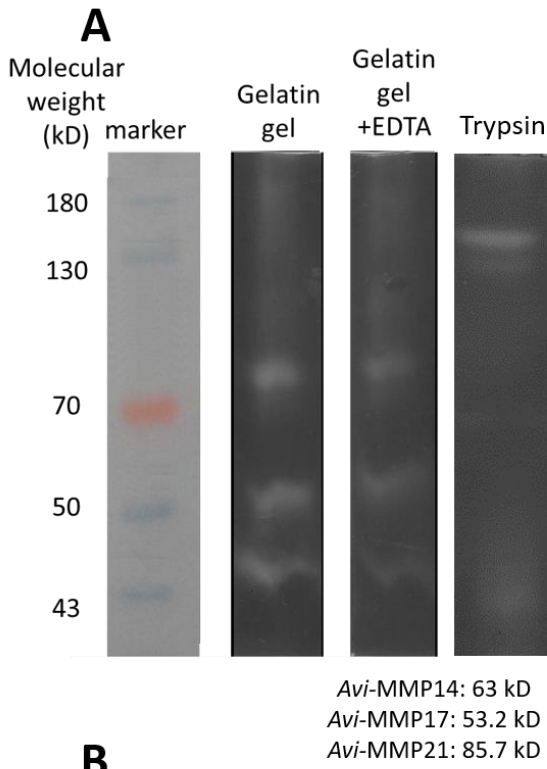
56

A

Avi-mmp2 (anterior regeneration)

0 hpa	6 hpa	12 hpa	24 hpa
10/10	9/10	10/10	8/10

48 hpa	72 hpa	96 hpa	120 hpa
9/10	10/10	10/10	10/10

B

Avi-mmp2 (anterior regeneration)

0 hpa	6 hpa	12 hpa	24 hpa
10/10	9/10	10/10	8/10

48 hpa	72 hpa	96 hpa	120 hpa
9/10	10/10	10/10	10/10

Figure 7: *Avi-mmp21* expressing localization during the anterior regeneration.

(A) *Avi-mmp21* expressing localization in the regenerating worms. Sense probe was used as negative control. (B) During the anterior regeneration, gene expression of *Avi-mmp17* can be observed in the blastema after 6 hpa. The gene expression increased to maximum at 24 hpa and 48 hpa. Then, the gene expression decreased after 72 hpa. The gene expression decreased to normal level after 96 hpa. The red dah line is the cutting line. The number at bottom left is the ratio of showed photos in the sample. Scale bar: 100 μm.

A

Molecular weight (kD) marker

Gelatin gel

Gelatin gel +EDTA

Trypsin

180

130

70

50

43

Avi-MMP14: 63 kD
Avi-MMP17: 53.2 kD
Avi-MMP21: 85.7 kD

C

Relative gelatinolytic acitivity

regeneration time point

Intact 0 hpa 12 hpa 24 hpa 48 hpa

B

Molecular weight (kD) Marker intact 0 hpa 12 hpa 24 hpa 48 hpa

250

180

70

50

43

34

20

1

2

3

59

Figure 8: Zymograph showed the active MMPs in *A. viride* during regeneration.

(A) The zymograph showed that three clear bands, 80 kD, 55kD and 45kD, which suggests three gelatinolytic enzymes exist in the crude extract proteins in *A. viride*. They might be Avi-MMP21, Avi-MMP14 and Avi-MMP17, respectively. In the group treated with EDTA, all the three bands became unclear, which suggested that all these enzymes belongs to metalloproteinases. The trypsin group was used as positive control.

(B) The blastema of the early stage of anterior regeneration were collected to do the zymograph. It showed all these three MMPs are activated in the early stage of regeneration and their activity have a peak at 24 hpa. Then, their activity decreased to normal level. (C) The statistical data of the three bands in (B). All the three activity increased about two-fold higher than intact head. *: $p < 0.05$. **: $p < 0.01$.

A

B

144 hpa

1 % DMSO   200 μM GM6001

61

C

Amputation   24 hpa   48 hpa   72 hpa   96 hpa   120 hpa   144 hpa

Treatment   1 % DMSO   200 μM GM6001 in 1 % DMSO

control
0-12
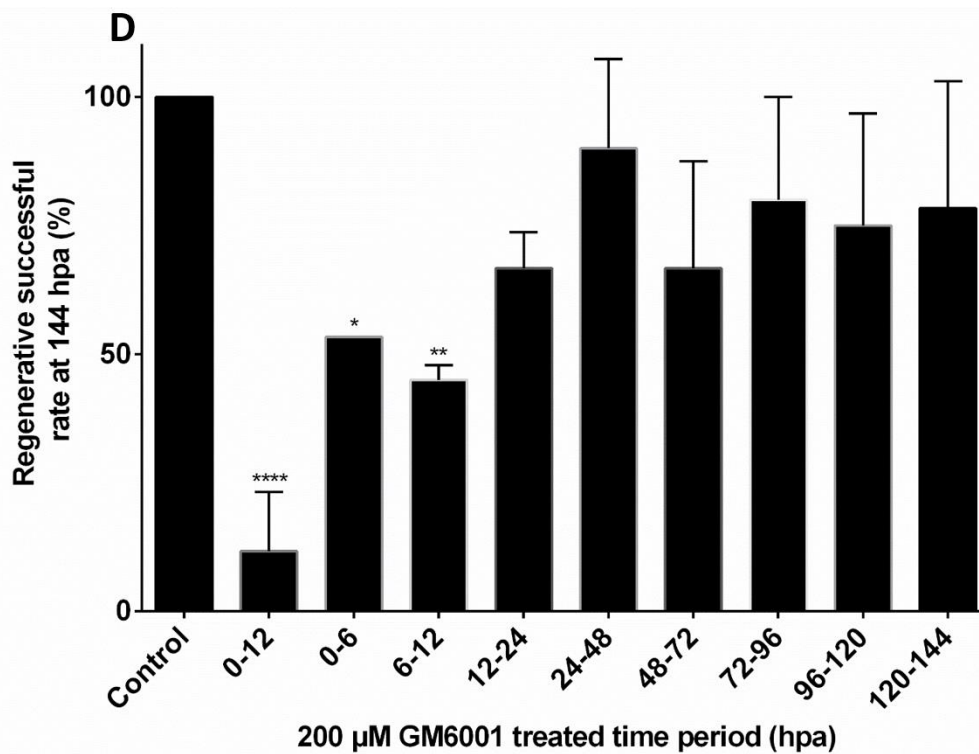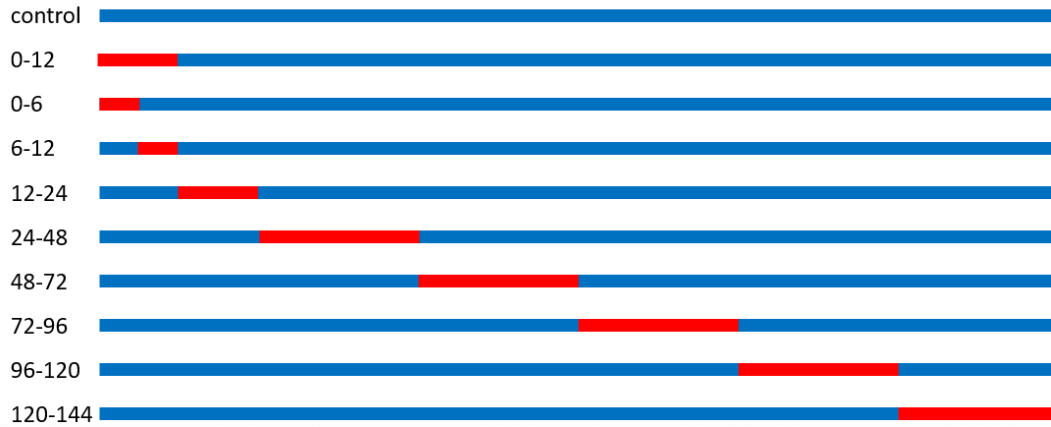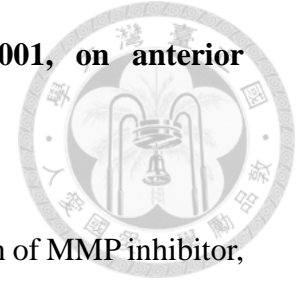0-6
6-12
12-24
24-48
48-72
72-96
96-120
120-144

D
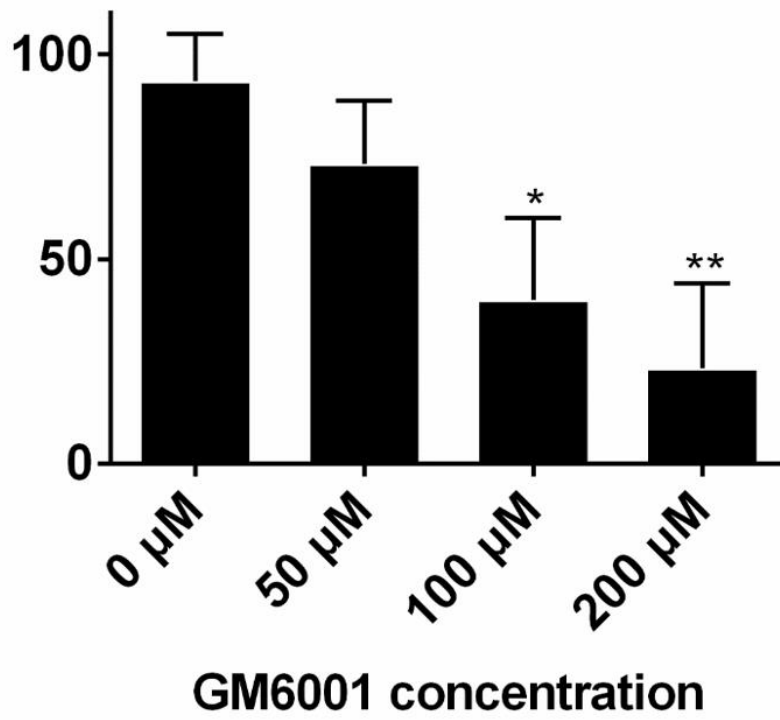
Figure 9: The inhibitory effect of MMP inhibitor, GM6001, on anterior regeneration in *A. viride*.

(A) The amputated *A. viride* was treated with different concentration of MMP inhibitor, GM6001, to see what its effects on regeneration is and whether MMPs is involved in the regeneration. The regeneration successful rate at 144 hpa was measured. It showed the dose-dependent inhibition effect of GM6001. When treated with 200 μM of GM6001 the regeneration successful rate significantly decreased to about 20 %. (B) The photos are the amputated *A. viride* at 144 hpa. In the group without GM6001, the anterior regeneration completed with functional head. However, in the group treated with 200 μM of GM6001, most of the regeneration failed. Some of the worms were stuck at wound healing stage, which showed little or no blastema. And, others became cysts and lay dormant until they die. (C) The different treatment in (D). The arrow shows the anterior regeneration in *A. viride*. The blue line shows the periods that amputated *A. viride* were immersed in the ASW with 1 % DMSO. The red line shows the periods that amputated *A. viride* were treated with 200 μM of GM6001. (D) To figure out whether the function of MMPs is time-dependent, *A. viride* was treated with GM6001 at different time period of regeneration. Although GM3001 has regenerative inhibition effects at 0-24 hpa. When treated with GM6001 at 0-6 hpa and 6-12 hpa, it showed about 50 % regeneration inhibition effects. Surprisingly, only when treated with

63

GM6001 at 0-12 hpa, the regeneration successful rate at 144 hpa significantly decreased

to 10-20 %. This results suggested that MMPs might play crucial roles in the 0-12 hpa.

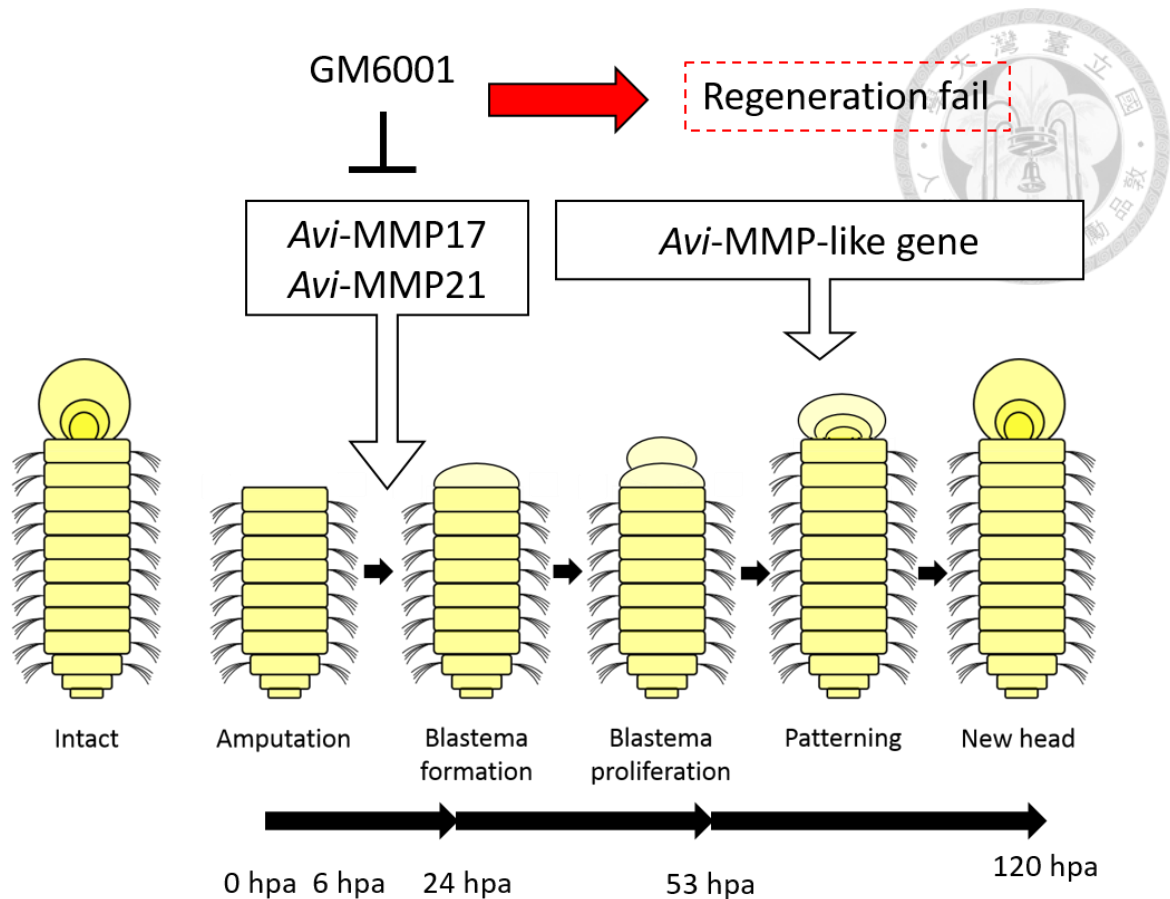*: $p < 0.05$. **: $p < 0.01$. ****: $p < 0.0001$.
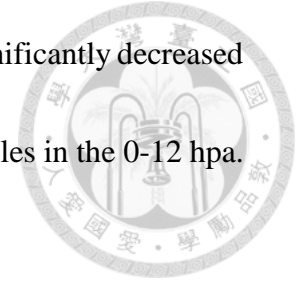
Figure 10: The model of MMPs involved in the anterior regeneration in *A. viride*.

In the previous studies done in our lab, it showed that the wound healing is completed at 6 hpa. The blastema can be observed after 24 hpa. And the mouth opening appeared at 53 hpa. Finally, the anterior regeneration completed at 120 hpa. During these regenerative processes, at least three MMPs was involved. Two of MMPs, *Avi*-MMP17 and *Avi*-MMP21, might play crucial roles in the early stage of anterior regeneration. After their activities were inhibited by MMP inhibitor, GM6001, the regeneration failed. And, the other one MMP, *Avi*-MMP-like gene, might be involved in the late stage of anterior regeneration.

Tables

Table 1: Primers used for cloning *Avi-mmp*

Primer	sequence
Avi-mmp14 1F	5'-CGACGATGTGGTGTGCCCGAC-3'
Avi-mmp14 1R	5'-CTTCCGGTAAAGGAGGGCGCG-3'
Avi-mmp14 2F	5'-GTAGCTCCCACCAGAACGACTCC-3'
Avi-mmp14 2R	5'-GTTCTATACTACTACCTTCAGTATTTAGGTGTGC-3'
Avi-mmp14 3F	5'-CTCATGCGACAGAATATACGCTTC-3'
Avi-mmp14 3R	5'-CGTACAATGCACAAGACATTATGCAC-3'
Avi-mmp14 4F	5'-CGGTTACTGCAGCACGAACGGTAC-3'
Avi-mmp14 4R	5'-GGTGATGTCGGGCACACCACATC-3'
Avi-mmp14 5'RACE 1	5'-GTAGACCTATACCAGGAATTTCAAGCG-3'
Avi-mmp14 5'RACE 2	5'-GGTTACTGCAGCACGAACGGTACAC-3'
Avi-mmp17 1F	5'-GCGTATTTCACTGCTTGTCAAATCCGG-3'
Avi-mmp17 1R	5'-GCAGCTGTCCCGACACATTTTGGC-3'
Avi-mmp17 2F	5'-GATACGTGCTCGGCCCGAGC-3'
Avi-mmp17 2R	5'-GGCTTATGTATGTATGTATGCATATGCATG-3'
Avi-mmp17 3F	5'-GCGCGTGTTCGTGCGTTAATTC-3'
Avi-mmp17 3R	5'-CATGCATGCACACAAACACGCAC-3'
Avi-mmp17 3' RACE 1	5'-GCTCGGCCCGAGCAAGTGG-3'
Avi-mmp17 3'RACE 2	5'-GAAGGCAGCGCCGATACGTGC-3'
Avi-mmp-like gene 1F	5'-GGATAACGAATGCCAGTTACATCGGC-3'
Avi-mmp-like gene 1R	5'-CTACGACAGCGTCACCCAAATATACAAC-3'
Avi-mmp-like gene 2F	5'-CCAGAACTGCTCCGTCCTC-3'
Avi-mmp-like gene 2R	5'-CGCTGGTTTCGATACTTCCAG-3'
Avi-mmp-like gene 3'RACE 1	5'-GTGTGAACTGTTGTATATTTGGGTGACGC-3'
Avi-mmp-like gene 3'RACE 2	5'-GACCGCGGTGAAAATACAGCACTGTC-3'
Avi-mmp-like gene 3'RACE 3	5'-CCAACGTGGATTATCCATCCAGTCC-3'
Avi-mmp21 1F	5'-GCCTTGGCTCATCTACGCTCATTAC-3'
Avi-mmp21 1R	5'-CATCGGAAACCTCTGCTTCTTCAGC-3'
Avi-mmp21 2F	5'-GCTCATCTACGCTCATTACAGC-3'
Avi-mmp21 2R	5'-GACATATGATCACGTAATGAGGCG-3'
Avi-mmp21 3F	5'-CGCGTGGCCAACGAAGAAATGGC-3'

Avi-mmp21 3R	5'-GATCACGTAATGAGGCGATGATGCAG-3'
Avi-timp1 1F	5'-GTATGTGTGTATGTATGTATATATGTATGTAG-3'
Avi-timp1 1R	5'-CTGTATAAAGTCACGTGACAACTACTGC-3'
Avi-timp1 2F	5'-CGCTTTGGTTTAGGCGGTGGTAGC-3'
Avi-timp1 2R	5'-CATGCCGCAGCATTCACAGACAGC-3'

Table 2: Primers used for the RNA probes

primer	sequence
Avi-mmp14 ISH 1F	5'-GCATTTACTAATGCCTTGAAAGGCG-3'
Avi-mmp14 ISH 1R	5'-CTATATTAGTCTCTGTAATGTAACATC-3'
Avi-mmp17 ISH 1F	5'-CCTGGAACTGTACTTGCTCATGCCTATC-3'
Avi-mmp17 ISH 1R	5'-GCCAGCCTCTCTCACATTCATCTTGAC-3'
Avi-mmp21 ISH 1F	5'-CGGGCCTTCTCGTAACATGCTTGTG-3'
Avi-mmp21 ISH 1R	5'-GGGCCTATCTGGAAACACTTAAACTCGTG-3'
Avi-mmp21 ISH 2F	5'-GCCTTGGCTCATCTACGCTCATTAC-3'
Avi-mmp21 ISH 2R	5'-GAACTGCTCCATTATTGCCTACCTCATG-3'
Avi-timp1 ISH 1F	5'-CTTTGGTACCAATGTTGGTGTTATTGTTTGC-3'
Avi-timp1 ISH 1R	5'-GGCGGTGGTAGCTGGTTTCAC-3'
Avi-timp1 ISH 2F	5'-GGCGGTGGTAGCTGGTTTCAC-3'
Avi-timp1 ISH 2R	5'-CTGTATAAAGTCACGTGACAACTACTGC-3'

Table 3: Primers used for qPCR

Primer	sequence
Avi-mmp14 qPCR F	5'-GTGACCAGACACCGCTTATT-3'
Avi-mmp14 qPCR R	5'-TACACCGGGTCCATCAAATG-3'
Avi-mmp17 qPCR F	5'-CGTCATCAACTTCTCAGCCTA-3'
Avi-mmp17 qPCR R	5'-CCTGTGATGAGACGAACTGAAG-3'
Avi-mmp-like gene qPCR F	5'-TCAACCTCGACTTCATTTCCTT-3'
Avi-mmp-like gene qPCR R	5'-ATACATAGCGCGTGGTTCTG-3'
Avi-mmp21 qPCR F	5'-TCAGACGACAGCTCACAAAG-3'
Avi-mmp21 qPCR R	5'-GGCCGAGTACATGACCTATTT-3'
Avi-timp1 qPCR F	5'-GGACATCACCTTGGCTCTTATC-3'
Avi-timp1 qPCR R	5'-CGCTGTTCATTCTCCCTACTG-3'